General Disclaimer

One or more of the Following Statements may affect this Document

- This document has been reproduced from the best copy furnished by the organizational source. It is being released in the interest of making available as much information as possible.

- This document may contain data, which exceeds the sheet parameters. It was furnished in this condition by the organizational source and is the best copy available.

- This document may contain tone-on-tone or color graphs, charts and/or pictures, which have been reproduced in black and white.

- This document is paginated as submitted by the original source.

- Portions of this document are not fully legible due to the historical nature of some of the material. However, it is the best reproduction available from the original submission.

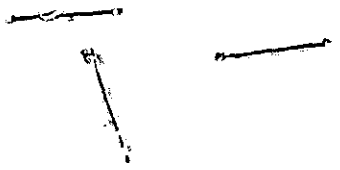

JET PROPULSION LABORATORY

CALIFORNIA INSTITUTE OF TECHNOLOGY

PASADENA, CALIFORNIA

N70-11900

(ACCESSION NUMBER)	(THRU)
94	1
(PAGES)	(CODE)
CR-106993	22
(NASA CR OR TMX OR AD NUMBER)	(CATEGORY)

FACILITY FORM 602

C9-10F

GESP-7011
MAY 1969

A DESIGN STUDY FOR A THERMIONIC REACTOR POWER SYSTEM FOR A NUCLEAR ELECTRIC PROPELLED UNMANNED SPACECRAFT

This work was performed for the Jet Propulsion Laboratory, California Institute of Technology, sponsored by the National Aeronautics and Space Administration under Contract NAS7-100.

NSP NUCLEAR SYSTEMS PROGRAMS
ISOTOPE POWER SYSTEMS OPERATION

GESP-7011
MAY 1969

A DESIGN STUDY FOR A THERMIONIC REACTOR POWER SYSTEM FOR A NUCLEAR ELECTRIC PROPELLED UNMANNED SPACECRAFT

QUARTERLY PROGRESS REPORT NO. 1

COVERING THE PERIOD 4 FEBRUARY 1969 TO 5 MAY 1969

MAY 23, 1969

PREPARED UNDER CONTRACT JPL 952381

FOR

ENERGY SOURCES GROUP

PROPULSION RESEARCH AND ADVANCED CONCEPTS SECTION
JET PROPULSION LABORATORY
4800 OAK GROVE DRIVE
PASADENA, CALIFORNIA, 91103

ISOTOPE POWER SYSTEMS OPERATION

GENERAL ELECTRIC
MISSILE AND SPACE DIVISION

P.O. BOX 8661
PHILADELPHIA, PENNA., 19101

ABSTRACT

This report discusses the technical progress of a design study program on thermionic reactor power systems for nuclear electric propelled, unmanned spacecraft. The purpose of this program is to provide designs of selected thermionic power systems integrated with nuclear electric unmanned spacecrafts over the range of 70 to 500 kWe. The basic program task structure and key guidelines are presented. Detailed characteristics of the mercury ion thruster, science payload and communications subsystems are given. Titan III C/7 launch vehicle restraints on shroud size and payload capability are discussed, and a point-of-departure 300 kWe powerplant design concept is developed in sufficient detail to permit initiation of preliminary analyses of spacecraft weight distributions and activated coolant dose rates. An evaluation of heat rejection systems shows that a two-loop system (the reactor coolant loop in series with the radiator coolant loop, with an intermediate heat exchanger) is approximately 550 pounds heavier than a single-loop system. A coolant activation analysis, based upon a bonded wet cell trilayer reactor powerplant, demonstrates that the two-loop spacecraft power system will be required.

TABLE OF CONTENTS

LIST OF ILLUSTRATIONS

LIST OF TABLES

LIST OF TABLES (CONT)

1. INTRODUCTION

A design study program of thermionic reactor power systems for nuclear electric propelled, unmanned spacecraft was initiated by the General Electric Company on February 4, 1969 for the Jet Propulsion Laboratory under Contract Number JPL 952381. The purpose of this program is to provide designs of selected thermionic reactor power systems integrated with nuclear electric unmanned spacecrafts over the range of 70 to 500 kWe unconditioned power. The key design objective is a weight of 10,000 pounds, including reactor, shielding, structure, power conditioning, and thruster subsystems at a 300 KW(e) unconditioned power level. Spacecraft propulsion will be provided by mercury electron bombardment ion thruster engines.

The program is divided into five principal tasks.

a. Task 1 - System Requirements and Evaluation - The purpose of this task is to establish program guidelines, program functional design requirements and system evaluation criteria.

b. Task 2 - Spacecraft Design - The purpose of this task is to prepare basic spacecraft designs for a Jupiter orbiter mission. Preliminary design layouts of the major spacecraft components and structural analyses of the supporting structure will also be included in this task.

c. Task 3 - Power Plant Design - The purpose of this task is to design and optimize the thermionic reactor power plants for each of three candidate reactor concepts (Gulf-General Atomics, General Electric, and Fairchild-Hiller).

d. Task 4 - System Analysis Development - The purpose of this task is to develop the necessary analytical procedures and computer codes required to conduct power plant design and optimization calculations and to perform parametric studies.

e. Task 5 - Mission Engineering - The purpose of this task is to prepare preliminary definitions of pre-launch, launch and mission operations, and to assess the possible impact of aerospace nuclear safety requirements upon power plant design.

The design study is performed in two consecutive phases:

a. Phase I - Design of unmanned spacecraft configurations, including power plants, for each of the three candidate thermionic reactor concepts. Key ground rules include:

   1. 300 KWe unconditioned power
   2. NaK-78 coolant
   3. 1350°F reactor outlet temperature
   4. Copper-stainless steel conduction fin radiators
   5. 10,000 pound power plant weight (design objective)
   6. 10,000 to 15,000 full power hours.

b. Phase II - Investigation of the effect of key parameters on power plant design:

   1. Power level: 70 to 500 KWe
   2. Coolant: substitution of lithium for NaK-78
   3. Radiator type: the use of vapor fin radiators
   4. Extended life: 20,000 full power hours
   5. Beryllium-stainless steel radiators.

Program effort is progressing well, and is currently on schedule. A key Phase I milestone has been completed with the selection of a two-loop primary heat rejection system. Launch vehicle-payload interfaces and minimum payload and communications subsystems have been defined. Point-of-departure designs showing preliminary estimates of radiator areas, component weights, and system weight distributions have been completed. Radiator configuration selection and spacecraft parasitic structural analyses are in progress and should be completed on schedule.

2 TECHNICAL DISCUSSION

The presentation of the following material follows the program task structure as outlined in Section 1. The results of the study to date are summarized in Section 3, Conclusions, and Section 4, Recommendations.

2.1 SYSTEM REQUIREMENTS

Program guidelines and functional design requirements have been identified. Key items are summarized below:

Phase I

1. A design objective shall be 10,000 lb total propulsion system weight including shielding, structure, power conditioning, and thruster systems for the 300 KWe reference design.

2. The spacecraft design shall define all primary and auxiliary systems including, but not limited to:

Reactor Shielding	Power Conditicning
Primary Radiator	Bus Bars
Primary Pump	Piping
Auxiliary Radiators	Spacecraft Structure
Auxiliary Pumps	Startup System

3. The spacecraft system shall be designed for launch by the Titan III C/7, and shall be compatible with the launch environment of this vehicle.

4. The reference point for the launch vehicle/spacecraft interface shall be 30,000 lb delivered into a 750 nm circular orbit.

5. The reference mission is a Jupiter planetary orbiter. Starting from the 750 nm circular orbit the 30,000 lb spacecraft will spiral away from earth ($\sim$ 50 days) and begin the trip to Jupiter. The following times and power levels are applicable.

Mission Mode	Power Level (kWe)	Time (days)
Initial Thrust	300	210
Coast	30	120
Final Thrust	300	270
Jupiter Orbit	30	(one orbit, 17 days minimum)

6. The meteroid model will be developed from the following models (definitions and assumed values are given in Section 5.0).

   a. Penetration Model:

$$t = 0.5m^{.352} \rho_m^{1/6} V^{.875}$$

   b. Meteoroid Flux

$$\phi = \alpha . m^{-\beta}$$

   c. Probability of Penetration

$$P(0) = \rho^{-\phi \cdot A \cdot T}$$

   d. Effective Thickness

$$t_{eff} = 0.432 \times t \text{ (Jupiter)}$$

7. The reference design shall be based on:

   a. NaK 78 coolant at 1350°F reactor outlet temperature,

   b. Electromagnetic pumps,

   c. Payload, power conditioning, and communications shielded to 10^{12} NVT > 1 mev, and 10^7 rad γ. Credit should be taken for attenuation from nonshielding materials.

   d. 14,500 lb of mercury propellant

   e. A stainless-steel tube, copper fin nondeployable radiator.

8. Power Conditioning:

   a. The power conditioning concepts identified in the reactor design studies will be evaluated and power conditioning systems will be defined which meet systems requirements.

   b. Reactor control concepts (constant voltage or constant emitter temperature) will be those specified by the reactor contractors.

9. Payload and Communications:

   a. The total payload and communications system will be assumed to weigh 2200 lb.

   b. The total power requirement for this system is assumed to be ~1 kWe. Electrical component temperature limit is 200°F.

10. Since reliability of individual components is unknown at this time, a reliability goal will not be established for the spacecraft. Emphasis will be placed on suitable configuration, light weight, careful design, and good engineering judgement.

11. The depth of study on "Mission Engineering" will depend on timely progress of the overall study, and shall be at the discretion of JPL, except that definition of launch vehicle characteristics shall be provided.

Phase II

The Phase II effort will be performed in the following priority:

1. Estimate system weight versus output power over the range of 70 to 500 kWe gross unconditioned power.

   a. Examine the system design modifications required if the General Electric "flashlight" reactor design is replaced by a GGA "dry flashlight" reactor design, if data are provided by the AEC.

   b. Determine the feasibility of placing a 70 kWe thermionic electric propulsion spacecraft aboard the Titan IIIF/Centaur launch vehicle.

2. Determine effect on system weight of varying NaK outlet temperatures in the range 1200° to 1500°F.

3. Examine the use of Li vs NaK-78 coolant. Treat startup considerations and payload shielding effects in detail.

4. Compare conventional versus vapor fin radiators on a weight basis.

5. Examine the system effect of a bonded trilayer in the General Electric reactor.

6. Document the computer program evolved to estimate the effects of major parameter variation, e.g., integrated dose, system pressure drop, and radiator temperature, on system weight.

7. Determine the effect of reactor output voltage on power conditioning, weight, temperature and efficiency.

8. Use of beryllium in the finned radiator for meteoroid protection.

9. Effect of extended life.

10. Determine the effect of changing the non-puncture probability to 0.99 on the 300 kWe General Electric and GGA designs.

11. Determine the effect on overall system weight of using a dynamic system for power conditioning the 300 kWe reactor system.

12. Determine the effort on auxiliary radiator system weight of using heat pipes to transmit heat to the radiator surface. Use the auxiliary radiator designed for cooling the General Electric static power conditioner.

2.2 SPACECRAFT DESIGN

2.2.1 Subsystem Definition

Characteristics of the thruster, science payload, communications and thermal control subsystems have been identified. These systems will be common to each of the three thermionic reactor spacecraft concepts.

2.2.1.1 Thrusters - Spacecraft propulsion will be provided by 31 equal size electron bombardment ion thruster engines. Mercury was chosen over other propellants because of the present relatively well developed technology of mercury systems. Information concerning the weight, volume, and position requirements of the thruster subsystem has been specified by JPL. The general guidelines used to design the thrust subsystem are given in Table 2-1.

Six spare thrusters will bring the total to 37 units. Considering switching and power conditioning requirements this number of spares provides one spare thruster for each group of five operating thrusters. Switching, logic, and spare power conditioning control (PCC) units can also be grouped in this way to reduce the number of

possible thruster - PCC combinations. Thrust vector control will be provided by a three axis attitude control system (two axis translation, one axis gimbal). Thruster power supply requirements and subsystem weights are given in Tables 2-2 and 2-3 respectively.

TABLE 2-1. GUIDELINES FOR THRUSTER SUBSYSTEM DESIGN

Power to the thrusters	240 kWe
True specific impulse	5000 sec
Thruster redundancy	20%
Attitude control	Electric propulsion
Maximum envelope diameter	10 feet
Thrust duration	10,000 hrs
Number of thrusters (includes 6 spares)	37

TABLE 2-2. ION ENGINE POWER SUPPLY REQUIREMENTS

				NOMINAL RATING						MAX RATING		
Supply Number	Supply Name	Type	Output(1)	Volts	Amps	Watts	Reg. %	Peak Ripple	Volts	Amps	Amps Limit(2)	Control Range, A
1	Screen	DC	V	3100	2.32	7200	1.0(V)	5	3200	2.32	2.60	2.0 - 2.4
2	Accelerator	DC	F	2000	.02	40	1.0(V)	5 @ 0.2 A	2100	0.20(3)	0.21	---
3	Discharge	DC	V	35	8.3	290	1.0(V)	2	150 @ 50 mA	9 @ 37V	10	7.5 - 9.0
4	Mag - Man	DC	F	15	.7	11	1.0(I)	5	20	1.0	1.0	---
5	Cath Htr(4)	AC	F	10	4.0	40	5.0	5	11	4.4	4.4	---
6	Cath Keeper	DC	F	10	0.5	5	1.0(I)	5	150 @ 50 mA	1.0 @ 20 V	1.0	---
7	Main Vapor	AC	V	0.6	1.0	1	Loop	5	8(5)	2.0	2.2	0.5 - 1.5
8	Cath Vapor	AC	V	0.3	0.5	1	Loop	5	8(5)	1.0	1.1	0.2 - 0.8
9	Neut Cath Htr	AC	F	10	2.0	20	5.0	5	11	2.2	2.2	---
10	Neut Vapor	AC	V	0.3	0.5	1	Loop	5	8(5)	1.0	1.1	0.2 - 0.8
11	Neut Keeper	DC	F	10	0.5	5	1.0(I)	5	150 @ 50 mA	1.0 @ 20 V	1.0	---

(1) V = Variable, F = Fixed

(2) Current limit or overload trip level

(3) Current at this level for less than 5 min. at low repetition rate.

(4) Needed only during startup or until discharge reaches 3A.

(5) Startup only.

TABLE 2-3. THRUSTER SUBSYSTEM WEIGHTS

Component	Weight (lbs.)
Thrusters (37)	585
Thrust Vector Control System	548
Miscellaneous (wiring, adapters, etc.)	100
TOTAL	1233

2.2.1.2 Science Payload and Communications Subsystem - The general size, power requirements and key capabilities of representative Science and Communications subsystems have been defined for a Jupiter orbiter mission. The major guidelines used in the selection of these systems are:

- The total electric power available to the science payload and communications subsystem is one kWe.
- The total weight allocated to the science payload and communications subsystems (including thermal control radiators for these subsystems) is 2206 pounds (one metric ton).

2.2.1.2.1 Science Payload Subsystem - A variety of experiments have been identified to provide answers to the basic scientific questions of interest in a Jupiter mission. A brief description of the science payload equipment is given below. Individual payload subsystem characteristics are summarized in Table 2-4. Total subsystem weight is 185 pounds and will require 87 watts of spacecraft power (all science operating).

Television System - In order to meet scientific objectives, particularly in terms of both high spatial resolution and large area coverage, a two-camera, slow scan vidicon television system with optics having 10:1 focal length ratio is assumed. Both cameras are identical except for lenses and shutters. The cameras are electromagnetically deflected and focused to obtain the spot size required for high resolution operation.

TABLE 2-4. SCIENCE PAYLOAD AND DATA HANDLING EQUIPMENT SUMMARY

COMPONENT	QUANTITY	UNIT CHARACTERISTICS					
		WEIGHT LBS.	DIMENSIONS INCHES	POWER (WATTS)	VOLTS	BIT RATE (SEC^{-1}) CRUISE	BIT RATE (SEC^{-1}) SPECIAL EVENT
PAYLOAD							
TV System							
Camera A (50 mm focal length)	1	7	9 x 5 x 4	---			
Camera B (508 mm focal length)	1	28.5	32 x 10 x 10	---			
Logic and Data Control	1	3	6 x 14 x 1.5	---			
Camera Drivers	1	4	6 x 14 x 1.5	---			
Data Converter	1	3	6 x 14 x 1.5	---			
Power Supply	1	4	6 x 7 x 2	32	28 VDC	---	1.5×10^6/picture
Infrared Spectrometer System	1	31(a)	6 x 10 x 8(b)	6	28 VDC	---	---
Ultraviolet Spectrometer	1	30	20 x 10 x 6(b)	12	28 VDC	---	---
Infrared Radiometer	1	5	6 x 6 x 6(b)	3	28 VDC		
Micrometeoroid	4	5	8 x 8 x 9	0.5	28 VDC	3	60
Interplanetary Fields							
Plasma	1	9.5	7 x 7 x 6	4.0	28 VDC	10	150
Cosmic Ray	1	5.0	9 x 7 x 6	2.0	28 VDC	10	40
Magnetometer	1	7.5	6 x 6 x 6	2.5	28 VDC	3	3
Electric	1	1.5	3 x 3 x 4	0.5	28 VDC	3	3
DATA HANDLING							
Digital Automation System	1	13.0	10 x 7 x 17	19.0	28 VDC	NA	NA
Data Storage System	1	10.0	12 x 12 x 12(b)	3.0	28 VDC	NA	NA
Command Decoder	1	3.0	9 x 6 x 2	1.0	28 VDC	256 Commands	
TOTALS	20	185.0	---	87.0	---	---	1.5×10^6

(a) includes gas system.
(b) estimated.

Infrared Spectrometer System - This equipment will acquire data concerning Jupiter surface composition, gas temperature, albedo, surface temperature, and atmospheric photochemistry. The infrared spectrometer telescope-monochromator weighs approximately 19 pounds. The gas system, consisting of two pressure vessels, weighs approximately 12 pounds and is also mounted on the scan platform. The power required by the infrared spectrometer is:

a. 4 W of 2.4-kHz square wave for the electronics during orbit

b. 2 W of 400 Hz square wave for the motor during orbit.

Ultraviolet Spectrometer - The scientific objective of this experiment will be to detect the presence of certain atoms, ions and molecules in the upper atmosphere of Jupiter. The total weight of the ultraviolet spectrometer is 30 pounds and requires 12 watts of spacecraft power. The dimensions are estimated to be 20 by 10 by 6 inches.

Infrared Radiometer - The scientific objective of this experiment will be to determine the temperature of the Jovian atmosphere. The total weight of the instrument is five pounds and its size is estimated at 20 x 10 x 6 inches. Three watts of power will be required.

Micrometeoroid Sensors - The meteoroid environment experiment will investigate the momentum, energy and spatial distribution of meteoroids in the interplanetary region, as well as probable changes in this distribution in the asteroid belts and near Jupiter. It is planned to incorporate four sensors on the spacecraft, located 90 degrees apart in the payload bay in order to minimize the dependence of this experiment on spacecraft orientation during the interplanetary propulsion mode. Each unit is eight by eight by nine inches, weighs about five pounds and requires two watts of electric power.

Interplanetary Fields - Table 2-4 has listed the approximate weight, size and power requirements of the experiments required to investigate various aspects of interplanetary and Jovian fields. However, the ability to conduct such measurements from an electrically propelled spacecraft remains to be established. Such measurements will be complicated by either the inherent magnetic field setup by the operating electric power plant, or by the use of electric propulsion, or both.

Data Automation Subsystem - The data automation subsystem will control and sequence the science instruments, accept and convert the raw data, code and format the data into frames, provide temporary (buffer) storage, and route the data to either the flight telemetry subsystem or the data storage subsystem for direct or delayed transmission to earth. This subsystem will include both the logic portion and the power converter, and will occupy a volume of 1190 cubic inches. It will weigh approximately 13 pounds and will consume 19 watts of power.

Data Storage Subsystem - This subsystem will provide buffering between the high rate at which data is acquired by the TV and other scientific instruments and the lower rate at which these data can be returned to earth (about 10^4 bits/sec). It is estimated that a storage subsystem with a capacity of 2×10^8 bits of data would weigh ten pounds, and occupy about one cubic foot of space. Total power requirements will be about three watts. Since a typical TV picture requires about 1.5×10^6 bits of storage, a system of this size will store about 100 pictures and have adequate capacity for simultaneous storage of raw data from the other science experiments.

Command Decoder - This system is required to provide on-board time sequenced event control in the spacecraft in time periods where this cannot be accomplished by the ground station, and to initiate particular events in the scientific payload or spacecraft operation upon command from the ground station. The representative unit selected for this function will provide for 256 descrete commands, will weigh three pounds and will require one watt of power. Further study is required to define the total command requirements and their distribution between the science paylcad and other spacecraft or power plant operations.

2.2.1.2.2 Communications Subsystems - The total science payload power requirement has been identified as 87 watts(e). Allowing for a possible 100 percent growth in payload power requirements, the remaining power available to the communications subsystem is approximately 800 watts (based on the one kWe limitation).

A low gain omnidirectional receiving antenna, a high gain transmitting antenna, and a transmitter comprise the communications subsystem. Characteristics of these components are summarized in Table 2-5.

The high gain antenna is nine feet in diameter, and paraboloid in shape. Its weight is estimated to be 31 pounds, including cabling. The deployment and pointing system is estimated to be eight pounds. The low gain antenna is approximately six inches in diameter by two inches in depth, and weighs about two and one-half pounds.

Power input to the communications subsystem will be 800 watts(e). Operating at an overall efficiency of 25 percent the power transmitted will be 200 watts, permitting a data rate of about 10^4 bits/second from Jupiter orbit. This estimate is based on a 120 foot diameter earth-based receiver antenna and the nine foot spacecraft transmitting antenna discussed above. It is estimated that the transmitter will weigh about 20 pounds and occupy a volume of 400 cubic inches. These requirements are based upon a 28 volt DC (± 5%) power input. Some weight could be saved if the spacecraft could supply 2000 Hz to 3000 Hz power directly to the transmitter.

TABLE 2-5. COMMUNICATIONS SUBSYSTEM CHARACTERISTICS

Low Gain Antenna (Receiving)	
Diameter	6 inches
Weight (including cable)	2.5 pounds
Deployment, lbs.	Negligible
High Gain Antenna (Transmitting)	
Diameter	9.0 feet
Weight, (including cable)	31.0 pounds
Deployment	8.0 pounds
Power Input	800 watts(e)
Power Transmitted	200 watts(e)
Bit Rate	10^4 bits/sec
Transmitter	
Weight	20.0 pounds
Geometry, inches	6 x 6 x 20

2.2.1.3 Thermal Control Subsystem - With 1000 watts(e) supplied to the communications and payload subsystems, approximately 800 watts(t) must be rejected by thermal radiation (Figure 2-1). To dissipate this quantity of heat, a 17 pound passive radiator with 16.6 ft^2 of surface area will be required. These estimates were based on the following assumptions:

a. 175°F maximum radiator surface temperature

b. A surface emissivity of 0.85 on a 60-mil thick aluminum radiator structure

c. 70 percent fin efficiency

d. Ten percent allowance on weight for fittings and structure.

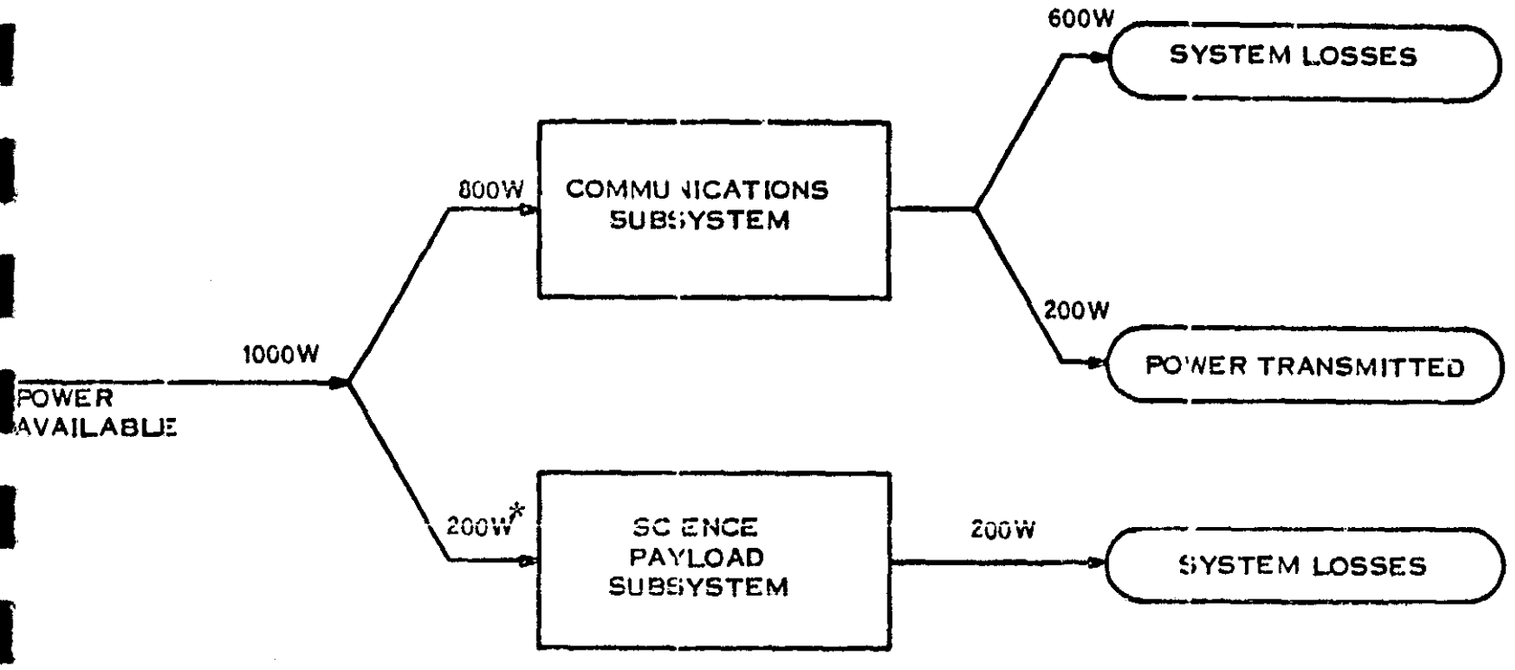

Figure 2-1. Electrical Power Distribution (Communications and Science Payload Subsystem)

2.2.2 Launch Vehicle Interface

The Titan III C/7 launch vehicle will be used to boost the spacecraft into a 750 nm (design objective) circular earth orbit. This vehicle is similar to the Titan IIIF except that it uses a standard transtage. It is a nonmanrated vehicle and employs the stretched Stage I tanks and seven segment, 120 inch diameter solids characteristic of the Titan IIIM. The overall length of the vehicle to the payload separation plane is approximately 117 feet.

2.2.2.1 Physical Constraints on Shroud Size - The height of the 50-ton bridge crane above the launch vehicle is one identified constraint on the aerodynamic shroud (hence payload) overall length. At the Eastern Test Range (ETR) Titan vehicles are launched from Launch Complex 40 or 41. With the Titan vehicle in place on the Mobile Service Tower, the clearance between the bridge crane and the Titan IIIC/7 payload interface is only 75 feet while for the Titan IIIC, this clearance is 88 feet. The decrease in available clearance is due to: (1) a 5-1/2 foot increase in the length of the first stage, and (2) a 7-1/2 foot increase in launch stand height. The launch vehicle contractor suggests the possibility of using ETR launch pad 37B, which has been used for S-IB launches. There would be virtually no height limitations.

On the launch pad, a universal environmental shelter is used to provide temperature and humidity control, and RF protection. It also acts as a clean room for the transtage and payload envelope. At the present time the limit of this facility is 55 feet, which means that this is the maximum payload plus transtage length which can be accommodated. Longer lengths will require major construction revisions to the shelter.

2.2.2.2 Flight Fairing Weight and Payload Penalty - During a "nominal" launch of the Titan III F vehicle, the flight fairing is normally jettisoned at 280 seconds, which is just after completion of the Stage I burn. In order to prevent freezing of the liquid metal coolant during launch, it may be desirable to retain the flight fairing as a radiation barrier until after reactor startup in earth orbit. However, this procedure imposes a severe payload weight penalty which depends on the shroud length (weight) and the terminal orbit altitude.

Figure 2-2 shows the flight fairing weight and the payload penalty as a function of shroud length, assuming shroud jettison at 280 seconds into the mission. If the shroud is retained past earth orbital insertion, then the payload weight penalty will be equal to the shroud weight. It should be noted that as the terminal orbital altitude increases, the payload penalty decreases for normal shroud ejection since a larger portion of the ΔV is added after shroud ejection. The curves are based on the data supplied by the Martin Marietta Corporation.

The effect of shroud retention on payload capability is shown in Figure 2-3. The upper lines define the Titan IIIC/7 payload capability for a 28.5 degree orbital inclination mission with shroud

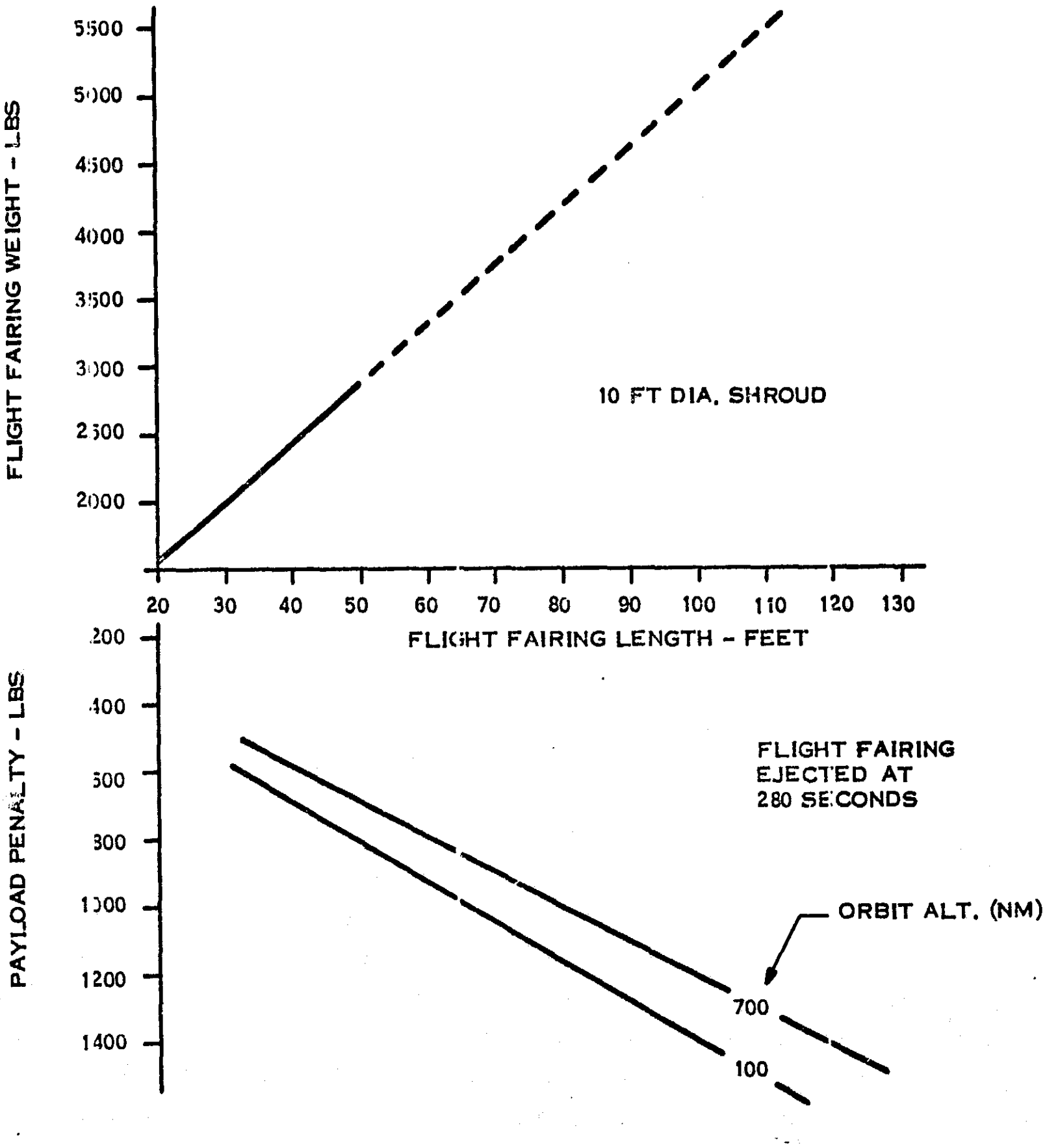

Figure 2-2. Flight Fairing Weight and Payload Penalty (Titan III C/7)

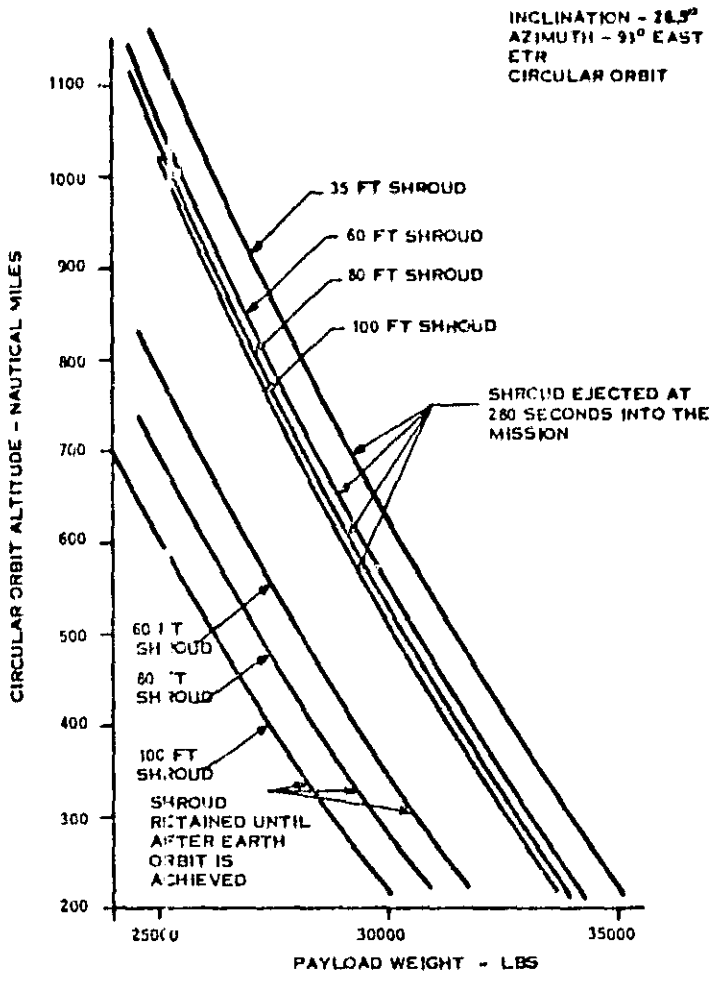

Figure 2-3. Effect of Shroud Retention on Payload Capability (Titan III C/7)

jettison occurring at 280 seconds into the mission. The lower curves show the effect of retaining the shroud through achievement of final Earth orbit.

Under nominal conditions, and with a 35-foot shroud, the vehicle can deliver 30,000 pounds into a 630 nm circular orbit. Employing longer shrouds, with jettison at 280 seconds, reduces the payload capability (initial mass in Earth orbit) as shown in Table 2-6a.

TABLE 2-6a. MAXIMUM PAYLOAD CAPABILITY WITH SHROUD EJECTION AT 280 SECONDS

Shroud Length (feet)	Shroud Penalty (pounds)	Maximum Payload Weight (pounds)
60	808	29,191
80	1021	28,978
100	1234	28,765

Alternatively, injecting 30,000 pounds of payload into circular orbit will decrease the maximum possible orbit altitude as shown in Table 2-6b.

TABLE 2-6b. MAXIMUM EARTH ORBITAL ALTITUDE FOR A 30,000 POUND PAYLOAD, WITH SHROUD JETTISON AT 280 SECONDS

Shroud Length (feet)	Maximum Orbit Altitude (nm)
60	555
80	530
100	512

If the shroud is jettisoned after achieving Earth orbit (630 nm), the payload capability will be reduced as shown in Table 2-6c.

TABLE 2-6c. MAXIMUM PAYLOAD CAPABILITY AT 630 nm WITH SHROUD EJECTION AFTER ACHIEVING EARTH ORBIT

Shroud Length (feet)	Shroud Penalty (pounds)	Maximum Payload Weight (pounds)
60	3300	26,700
80	4200	25,800
100	5000	25,000

2.3 POWER PLANT DESIGN

2.3.1 Point of Departure Power Plant

Power plant calculations were performed to define preliminary estimates of component weights and weight distributions. These point of departure estimates are required for evaluation of spacecraft structural requirements, one loop versus two loop studies, and radiator configuration studies. The design is based on the following assumptions:

a. A bonded wet cell trilayer diode reactor (13% reactor efficiency, 2010 kW reactor heat rejection).

b. An allowable power conditioning and payload electronics temperature level of 200°F; a corresponding radiator temperature of 175°F.

c. A power conditioning efficiency of 88 percent.

d. An effective meteoroid flux based on an averaged environment for a Jupiter mission. The resultant radiator armor reduction factor is 0.435, relative to Earth orbit missions.

e. A sink temperature of 300°R (approximate average for the entire mission).

f. Payload and communications subsystem weights are assumed to be 2000 pounds.

g. A copper-stainless steel conduction radiator.

h. A single loop primary heat rejection system.*

2.3.1.1 Primary Radiator - The main heat rejection loop is required to reject 2010 kW of energy utilizing a conduction fin stainless steel radiator with copper clad fins (Cu-SS) and NaK-78 coolant. The radiator is divided into two cylindrical bays with the circumference divided into two panels per bay; panel flow tubes are oriented parallel to the axis of the vehicle. An iron titanate coating is assumed to provide the radiator with an 0.9 emissivity.

The Cu-SS radiator data of Reference 1 (796 ft^2 optimized area limited case) was used as the basis for the radiator calculations. Based on 2101 kW of heat rejection, a radiator area requirement of 681 square feet was calculated with a corresponding radiator weight of 2860 pounds. This weight, however, was further reduced by a consideration of the following:

a. Reduced armor thickness due to the change in vulnerable radiator area.

b. Reduced armor thickness due to the Volkoff correction for the Jupiter mission average meteoroid flux.

*This effort was completed prior to the coolant activation analysis which, as presented in Paragraph 2.3.3, demonstrates that a two-loop primary heat rejection system is required.

c. Reduced bumpered armor thickness which is a function of the required armor thickness.

The required radiator armor thickness is proportional to the vulnerable area and is given by the following relationship:

$$t_k = A^{0.249}$$

At 796 ft^2, the required armor thickness is 0.163 inches. At 681 ft^2, the armor thickness is:

$$t_k = 0.163\ (681/796)^{0.249} = 0.157 \text{ inches.}$$

Applying the Volkoff armor thickness correction factor yields the minimum required armor thickness:

$$t_a = 0.435 \times 0.157 = 0.069 \text{ inches.}$$

The relationship between bumpered armor thickness and required armor thickness is shown in Figure 2-4 (Reference 2). Assuming a fin thickness of 0.045 inches (which is the optimized value reported in Reference 1 for similar radiator conditions), the fin thickness to required armor thickness ratio is 045/.069 - 0.65, which is outside the range of Figure 2-4. Therefore, assuming a conservative ordinate value of 0.8, the bumpered armor thickness is found to be 0.0133 inches. Rounding off, this is assumed to be 0.015 inches, yielding a corresponding total radiator weight of 1860 pounds. Table 2-7 summarizes the major characteristics of the primary radiator.

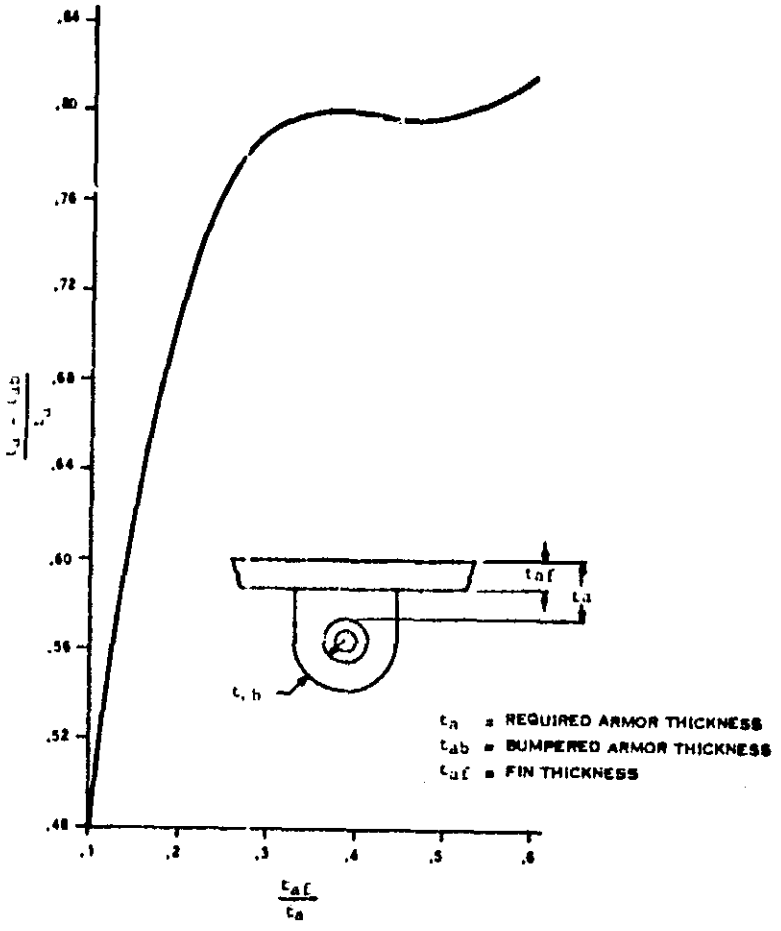

Figure 2-4. Meteoroid Armor Bumper Relationship

2.3.1.2 Power Conditioning Radiator - The power conditioning (PC) radiator consists of an array of square panels with a PC unit attached to each panel. Each panel dissipates the heat from a single PC module. In Figure 2-5, the PC module is attached to the

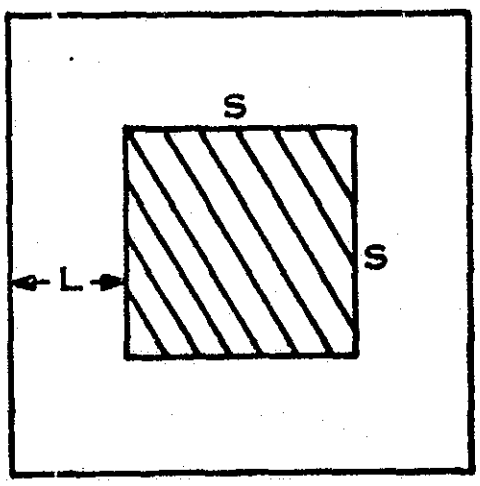

Figure 2-5. Power Conditioning Radiator Panel

TABLE 2-7 PRIMARY RADIATOR CHARACTERISTICS
(Point of Departure Power Plant, Single Loop)

Heat Rejection, Kw	2010
Radiator Weight, lbs	1860
Radiator Area, ft^2	681
Inlet Temperature, ^oF	1350
Fluid ΔT in Radiator, ^oF	180
Number of Panels	6
Panel Width, ft.	10
Number of Tubes per Panel	60
Tube, I.D., inches	0.250
Tube Length, ft.	11.1
Fin Thickness, inches	0.045
Required Armor Thickness, inches	0.069
Bumpered Armor Thickness, inches	0.015
Fin Length, inches	0.820
Coolant Flow Rate, lb/sec	51.2
Radiator ΔP, lb/in^2	6.52

central shaded section on the panel back side. Preliminary definition of the modules indicates that they will be approximately one foot square (S = 1). Limiting the module to this area is pessimistic from a heat rejection viewpoint because this limits the quantity of radiator area which operates at the maximum allowable temperature; however, dispersing the module components over the entire radiator area incurs weight penalties in additional electrical wiring. Since trade-off calculations were not performed for this point of departure design, the concentrated module arrangement shown in the sketch was assumed. The heat rejection penalties associated with this arrangement were offset somewhat by assuming one-dimensional heat conduction in the fin area.

The point of departure power conditioning radiator calculations were based on the following conditions and assumptions:

a. A maximum allowable radiator temperature of 175^oF (635^oR)

b. An average sink temperature of -160^oF (300^oR)

c. One hundred and twenty PC modules, approximately 110 of which are for low voltage power conditioning, and 10 for other special purposes.

d. A radiator fin thickness of .150 inches

e. A radiator surface emissivity of 0.88.

Radiator fin efficiency calculations were based on the 35.2 kW heat rejection reported in Reference 1. The fin efficiency (η_F) for unidirectional heat conduction in a fin is

$$\eta_F = \tanh (m L)/ mL$$

where L is the fin length. The overall surface effectiveness is given by

$$\eta_o = 1 - (1-\eta_F)(A_F'A)$$

The ratio of fin area to total radiator area, for S = one foot, is given by

$$A_F/A = 1 - \left(\frac{1}{1 + 2L}\right)^2$$

From thermal considerations, the required radiator area is given by:

$$A = q/\eta_o \xi \sigma (T_R^4 - T_S^4)$$

Assuming 120 modules (at 1 ft^2 each) the total base area ($A-A_F$) is constant at 120 ft^2, and the total radiator area requirement must satisfy the following geometric relationship:

$$A = 120/(1-A_F/A).$$

The calculational procedure is one of trial and error. Various values were assumed for the fin length (L) until the area determined by thermal requirements matched the area determined by geometrical considerations.

The radiator heat flux is:

$$\frac{q}{A} = \xi (\sigma T_R^4 - \sigma T_s^4) = h_r (T_R - T_s)$$

where h_r is assumed to be an equivalent heat transfer coefficient.

Evaluating h_r for the temperatures and surface emissivity of interest yields:

$$h_r = \frac{.88 (278.5 - 13.9)}{(635 - 300)} = 0.7 \frac{BTU}{hr\text{-}ft^2\text{-}^oF}.$$

Then,

$$m = \sqrt{\frac{2(.7)}{100\left(\frac{.15}{12}\right)}} = 1.06$$

Assume L = .59 feet, then

$$mL = 1.06\ (.59) = .626$$

and

$$\eta F = \frac{\tanh .626}{.626} = .886$$

The fin area fraction is

$$\frac{A_F}{A} = 1 - \left(\frac{1}{1+2\ (.59)}\right)^2 = .789$$

and the surface effectiveness is

$$\eta_o = 1 - .789\ (1 - .886) = .91$$

The radiator area required for heat rejection is found to be

$$A = \frac{35.2\ (3413}{.91(.88)(278.5-13.9)} = 568\ ft^2$$

and the area needed to satisfy the geometric constraint is

$$A = \frac{120}{1 - .789} = 568\ ft^2$$

Thus, the required area equalization has been achieved with a fin length of .59 feet.

Subsequent to the power conditioning radiator calculations, the efficiency of the power conditioning modules was lowered from 90 percent to 88 percent which is more representative of PC performance at low voltage reactor output. Rather than maintain the one square foot area per module assumption and take the large penalty in additional radiator fin area and weight, it was assumed that the module area was increased sufficiently to achieve a fin efficiency and fin area fraction as computed above. The the required total radiator area becomes:

$$A = 1.2\ (568) = 680\ ft^2$$

The total power conditioning radiator weight is 1540 pounds.

The performance of low temperature radiators are influenced greatly by sink temperature conditions. The 300°R sink temperature assumed for the PC radiator analyses is an approximate average for the entire flight, but 50 to 70 days will be spent in the spiral-out escape from Earth orbit where the sink temperature averages 455°R. The equations presented above were used to show that the PC radiator effective fin efficiency would decrease to 0.83 and the maximum operating temperature would increase to 212°F for the near Earth sink temperature environment. If it is imperative to maintain a 175°F maximum PC radiator temperature in orbit, then the system power level must be maintained below 77 percent of full power.

The heat rejection rate for the payload, high voltage leads and thruster PC totals approximately 3.2 kW. By ratio, the heat rejection area (at 175°F) is 52 ft^2 and the radiator weights total 114 pounds.

2.3.1.3 Primary Loop System - The weight of the primary loop system is dependent on the axial length of the power conditioning radiator which is located between the reactor-shield assembly and the main radiator. The change in vehicle axial length and the various radiator axial lengths were estimated in the following manner.

The total radiator area required aft of the shield is 1445 ft^2, which is 330 ft^2 greater than the design in Reference 1. In order to maintain a small shield half angle, the added area is assumed to be added in the form of right circular cylinder, placed at the aft end of the vehicle. The length of the cylindrical addition is 11.4 feet, resulting in an overall vehicle length of 78.5 feet, and an overall shroud length of 81.5 feet.

The increase in primary loop piping length is approximately 35 percent due to the change in PC radiator dimensions. With the added length, the optimum pipe diameter will decrease, however, the net change in piping weight will increase. This increase is estimated to be +25 percent, and since the piping accounted for 1000 pounds of the total primary loop weight in the original design, a 250 pound increase was assumed for the point of departure primary loop system. The primary loop weight is therefore 2090 pounds.

2.3.1.4 Low Voltage Cable - The average length of the low voltage cable has been increased by approximately 30 percent over the original design, increasing the cable weight to 890 pounds.

2.3.1.5 Payload - Revised estimates for the payload component weights indicate that the minimum scientific package will weigh about 185 pounds, the communications set will weigh 60 pounds, and 17 pounds will be needed for thermal control. The total minimum payload package weight is 262 pounds. However, in accordance with the design guidelines, the total payload weight, including communications subsystems is assumed to remain at 2200 pounds.

2.3.1.6 Thrusters - The total weight for the thruster subassembly has been estimated as 1233 pounds (Paragraph 2.2.1.1). This subassembly includes 37 thrusters, thruster vector control system, and miscellaneous hardware.

2.3.1.7 Weight Summary of the Point of Departure System - Initial power plant calculations were based on the assumption of cylindrical or conical shaped radiators. A summary of the weights for this system is given in Table 2-8. Additional calculations were made to determine spacecraft weight distributions assuming triform, cruciform, and flat panel radiator configurations. A summary of the weights for these systems are also given in Table 2-8. The weight distributions and component sizes are illustrated in Figures 2-6 through 2-9. Since these designs will be used, in part, to determine launch load structural requirements, no launch support structure weights are specifically included.

For similar temperature, and heat rejection rates, cylindrical and flat panel radiators have equal areas, but the triform and cruciform radiators require greater area because of lower effective view factors. The difference in geometry also results in different radiator lengths for the same radiator area and diameter envelope. The difference in lengths can be seen from the following ratios:

$$\frac{\text{Triform length}}{\text{Cylindrical length}} = 1.21$$

$$\frac{\text{Cruciform length}}{\text{Cylindrical length}} = 1.11$$

$$\frac{\text{Flat Panel length}}{\text{Cylindrical length}} = 1.57$$

These ratios were used to estimate total vehicle lengths, radiator lengths, and changes in piping lengths and weights, for the various radiator shapes.

TABLE 2-8. WEICHT SUMMARY, POINT OF DEPARTURE POWER PLANT SYSTEMS

	Cylindrical Configuration	Triform Configuration	Cruciform Configuration	Flat Panel Configuration
Power Plant - Total	15375	14790	15315	14935
Reactor	3100	3100	3100	3100
Neutron Shield	1500	1310	1415	1240
Gamma Shield	600	520	560	500
Radiator - Primary	1861	1860	2200	1575
- Power Cond.	1540	900	1095	780
- Auxiliary	90	90	110	75
- Payload	114	70	85	60
Coolant Loop - Primary	2090	2350	2215	2830
- Auxiliary	60	70	65	75
Power Conditioning-High Volt	2800	2800	2800	2800
-Spec. Duty	300	300	300	300
Power Cables - Low Voltage	890	980	930	1140
- High Voltage	280	290	290	310
Miscellaneous	150	150	150	150
Spacecraft Components - Total	2043	2043	2043	2043
Ion Engines	1233			
Propellant Tanks	810			
Payload (Science, Communication)	2200	2200	2200	2200
Total Spacecraft	19618	19033	19588	19178
Propellant	14500	14500	14500	14500
Initial Mass in Earth Orbit	34118	33533	34058	33678

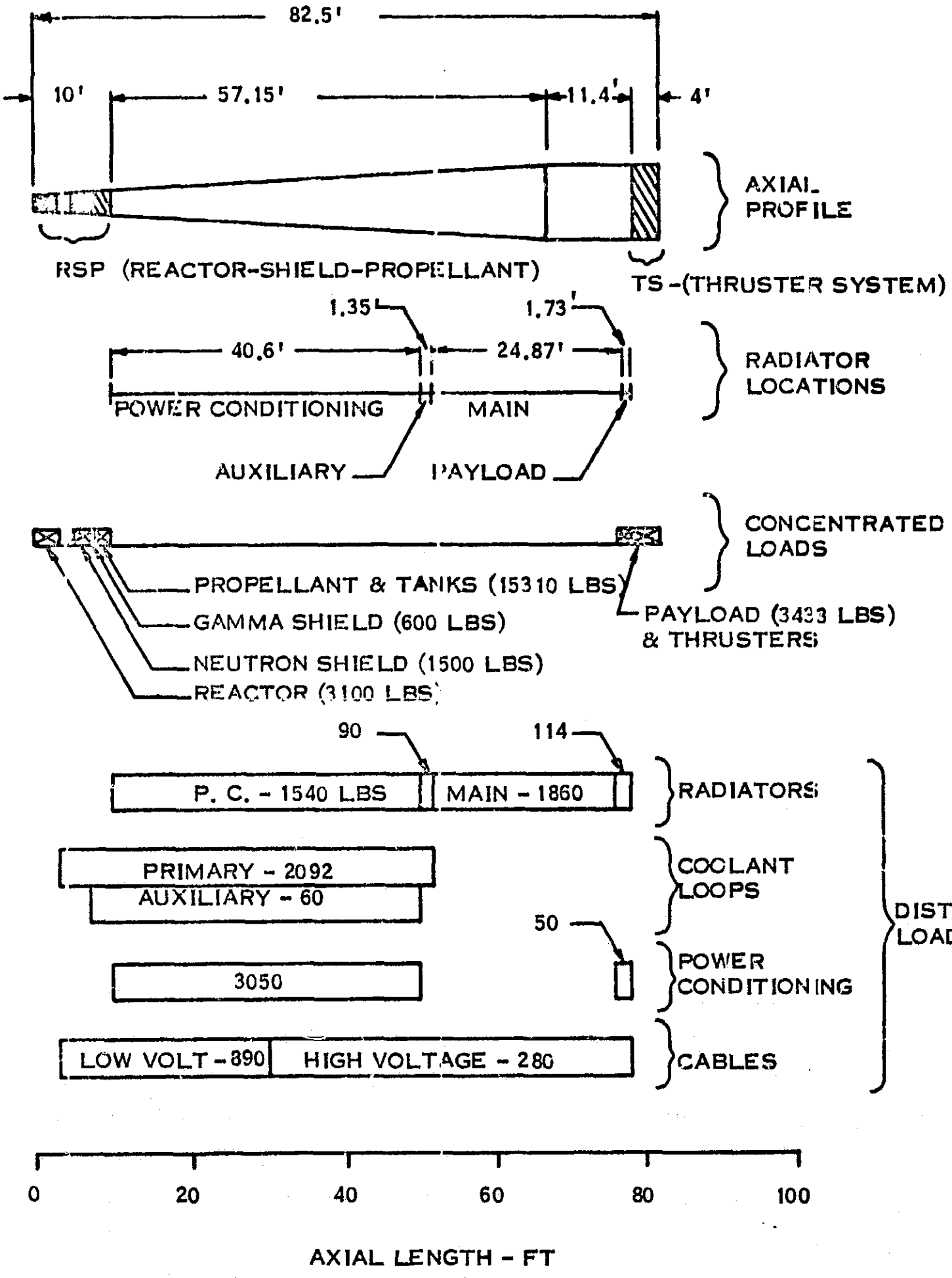

Figure 2-6. Reference Design-Cylindrical Radiator Configuration

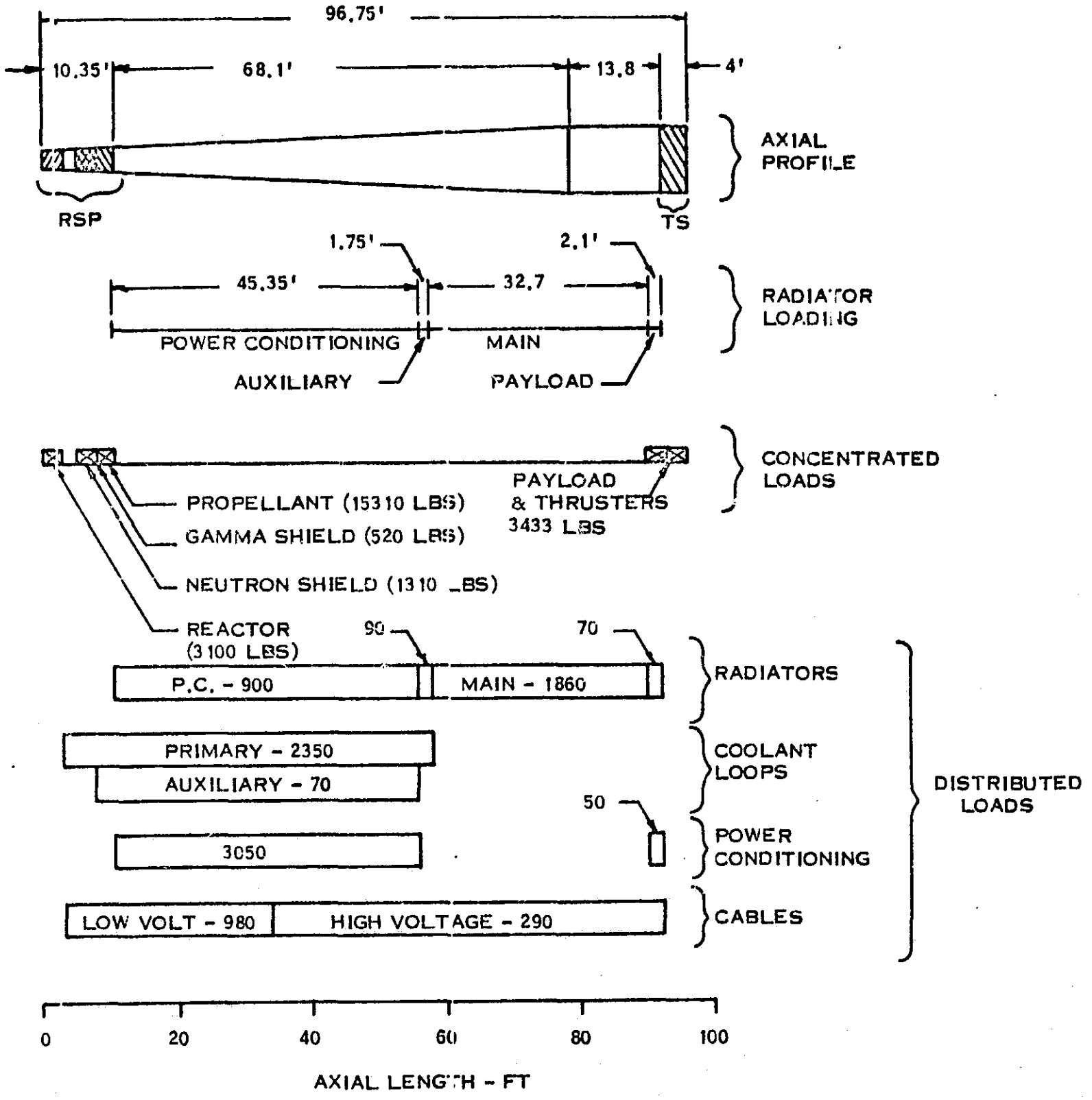

Figure 2-7. Reference Design-Triform Radiator Configuration

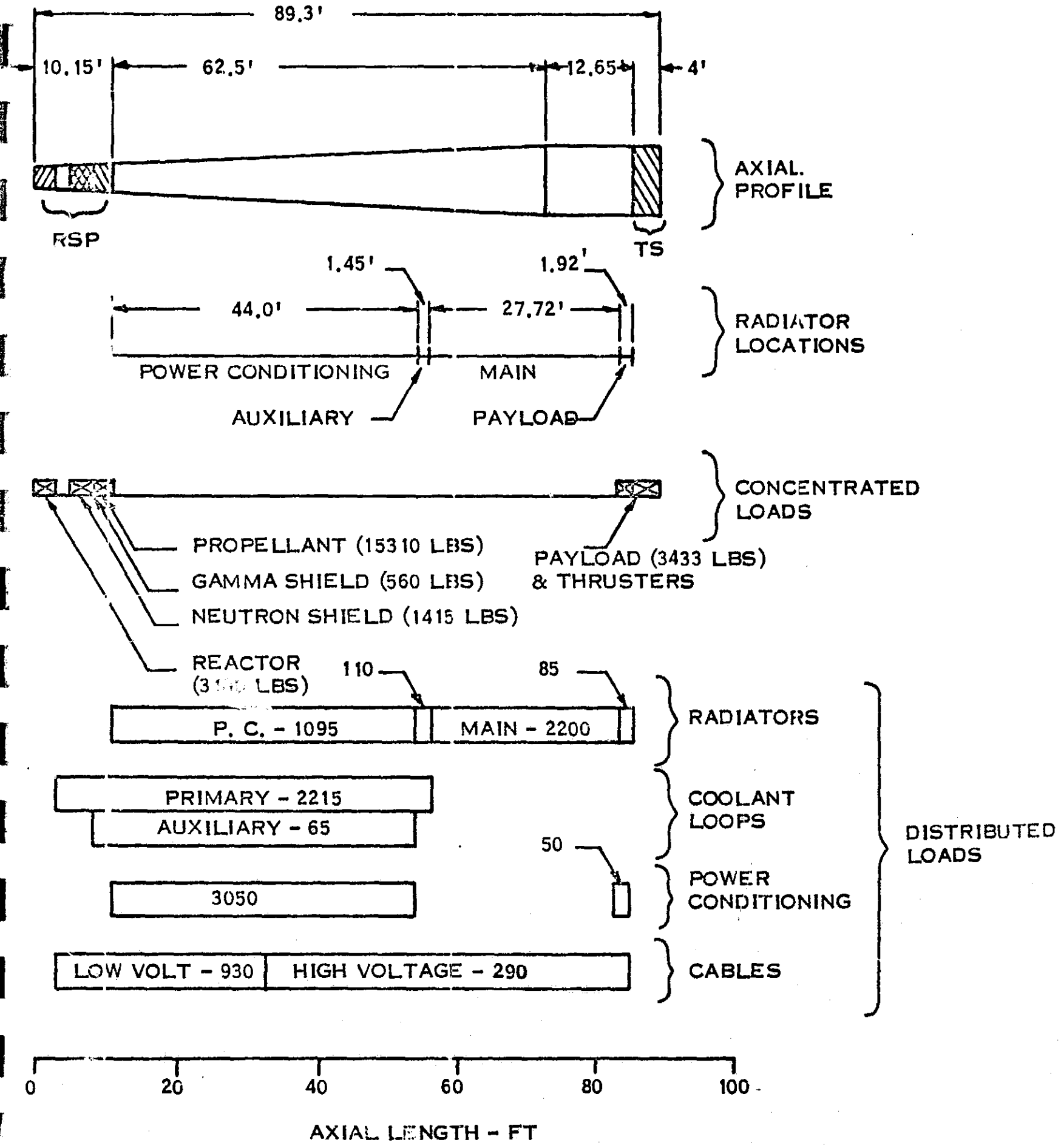

Figure 2-8. Reference Design-Cruciform Radiator Configuration

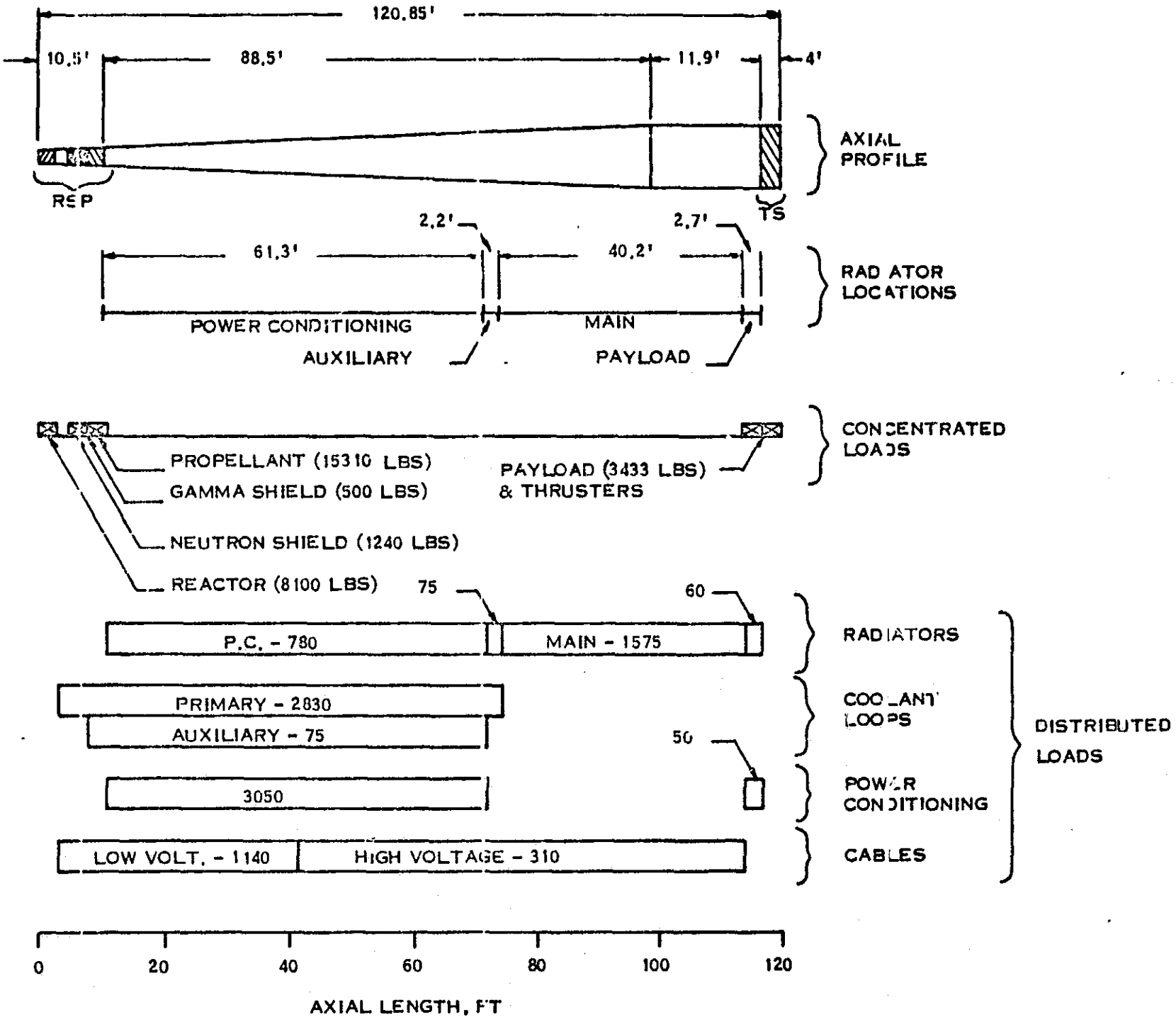

Figure 2-9. Reference Design-Flat Panel Radiator Configuration

As shown in Table 2-8, shield weights vary slightly as a function of radiator shape. The reason for this change is best described by an example corresponding to the flat panel radiator configuration. The shield must protect the payload and thruster assemblies which are positioned around the backface of the vehicle. The minimum diameter conical shield is therefore a function of relative placement of the reactor, shield and payload. However, the shield must also shadow the radiators to prevent radiation scattering back to the payload. The shape of this portion of the shield will be a slab having the same width as the cylindrical shield and a height sufficient to protect the radiator thickness. Figure 2-10 compares the cross sectional shape of the two shield components - the circular shield for payload thruster protection and the slab shield for radiator protection.

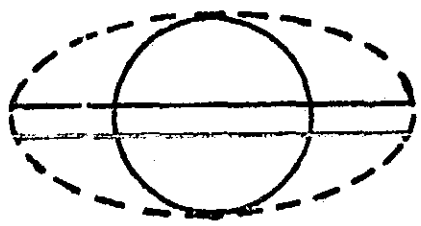

Figure 2-10. Example-Flat Plate Radiator Shield Geometry

The elliptical dashed outline illustrates the probable shape of the combined shield. This elliptical shape encompasses the areas of both the circular and slab shields, this geometry being required to prevent neutron or gamma radiation from being scattered into the payload or power conditioning areas behind the shield. Without the elliptical shape, radiation could be scattered out of the circular

shield before it is attenuated to the desired level and, for example, be further scattered from the slab shield into the payload area.

Shield volumes, normalized to the shield volume for the cylindrical vehicle configuration, were determined to be:

Triform/Cylindrical = .87

Cruciform/Cylindrical = .94

Flat Panel/Cylindrical = .83

The neutron and permanent gamma shield weights listed in Table 2-8 were computed directly from the above ratios.

2.3.2 Evaluation of A Two-Loop Heat Rejection System

Activated NaK-78 coolant is a major source of gamma radiation, particularly at collection points such as radiator header and feed line locations. In a single loop heat rejection system, the activated nuclei are distributed over large areas outside of the primary shields, and this source of gamma radiation, combined with contributions from the reactor and mercury propellant (secondary gamma source), determine the amount of local shielding required for power conditioning and payload electronic equipment. If radiation levels are excessive, a two-loop system may be used to confine the activated coolant within the reactor shield assembly. This is accomplished by locating the heat exchanger within the shield, preferably in a low neutron flux region to avoid excessive activation of the secondary loop. However, a weight penalty is incurred due to the addition of an intermediate heat exchanger, an additional pump, and a lower radiator inlet temperature. Figure 2-11 illustrates the two power plant concepts.

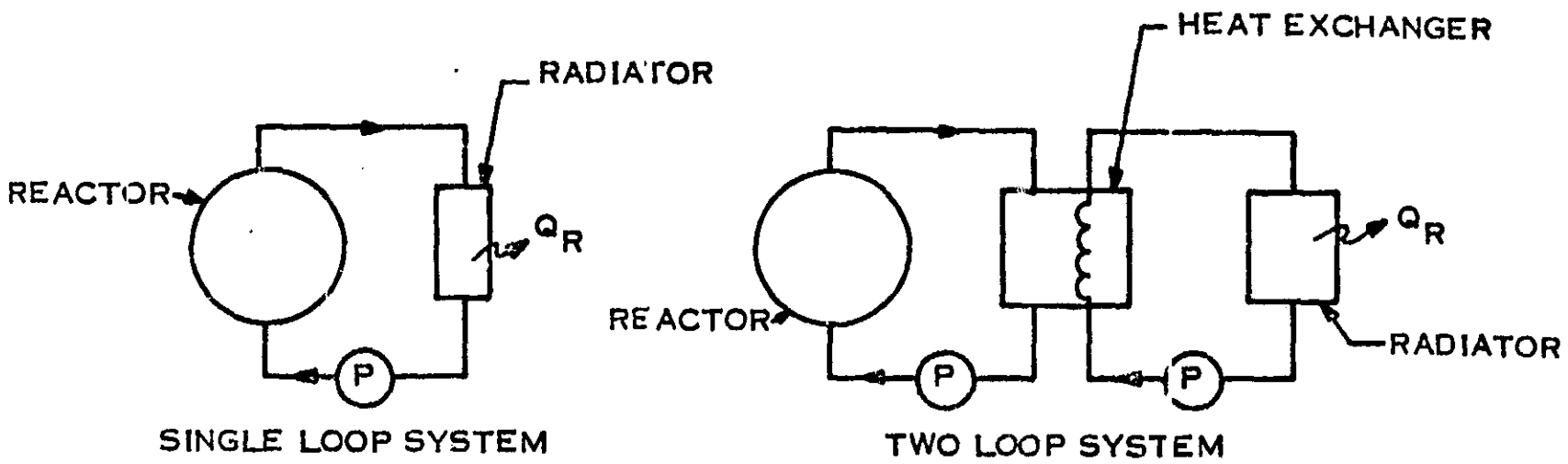

Figure 2-11. Single Loop and Two-Loop Power Plant Concepts

In the one loop concept, the radiator inlet temperature corresponds to the reactor outlet temperature, selected at 1350°F for this evaluation. Characteristics of this design are given in Table 2-7. In the two loop approach, the radiator inlet temperature is less than reactor outlet temperature. The weight of the heat rejection system depends upon the increased weight of radiator because of this temperature drop, the heat exchanger, and the additional pump. In general, as radiator inlet temperature approaches 1350°F, heat exchanger weight increases but both radiator weight and area decrease.

Assumptions used for the radiator calculations were the same as those used in the one loop calculations except that the radiator fluid temperature drop was varied in order to reflect the more complex system considerations. Because AC-EM pumps have higher reliabilities than DC pumps, it was assumed that an AC pump will be used in the secondary fluid loop. However, this assumption has only a minor effect on the total weight penalty.

Heat exchanger weights were based on a shell and tube stainless steel NaK to NaK design concept. The radiator coolant is assumed to occupy the tube side while reactor coolant flows in the shell side. The basic assumptions used in calculating the size and weight of the stainless steel heat exchanger are:

a. Inside tube diameter, 0.20 inch

b. Tube wall thickness, 0.020 inch

c. Tube flow velocity, 10.0 ft/sec

d. Shell flow velocity, 5.0 ft/sec

e. Shell wall thickness, 0.250 inch

f. Shell flow rate, 51.2 lb/sec

g. Tube flow rate, dependent upon radiator ΔT

The heat transfer resistance between the two fluids consists of the shell side boundary layer, stainless steel wall and tube side boundary layer. Due to the excellent heat transfer provided by the alkali metals and the minimal tube wall thickness, the overall heat transfer coefficient is approximately 2500 B/hr-ft^2-^{o}F. A logarithmic mean ΔT was used in order to calculate the required tube heat transfer area. Since the number of tubes is determined by the flow velocity and inside tube diameter, the length of the tubes is computed directly.

The heat exchanger weights given in Table 2-8 are based on the assumptions listed above and include fluid, tube, shell and end plate weight. In lieu of a specific design, the calculated heat exchanger weight was increased by 15 percent to account for fittings, header plates and baffles.

Table 2-9 summarizes the results of the two loop calculations. Since the heat exchanger weight is a small fraction of the radiator weight, the minimum system weight occurs at radiator inlet temperatures which approach reactor outlet temperature (1350^{o}F). Figure 2-12 shows the variation of two loop component weights and total system weight with reactor inlet temperature. The weight of a one loop radiator system was taken as 1860 pounds. It is seen that the minimum weight penalty associated with the two loop system is about 550 pounds.

TABLE 2-9. SUMMARY - TWO LOOP PRIMARY HEAT REJECTION SYSTEM CHARACTERISTICS

RADIATOR INLET TEMPERATURE (^{o}F)	RADIATOR FLUID Δ T (^{o}F)	RADIATOR WEIGHT AREA (LBS/FT^2)	HEAT EXCHANGER WEIGHT (LBS)	PUMP WEIGHT (LBS)	TOTAL WEIGHT (LBS)	2 LOOP SYSTEM WEIGHT PENALTY (LBS)
1345	250	1860/759	367	250	2477	617
1340	250	1840/770	277	250	2417	557
1320	250	1940/805	172	250	2412	552
1300	250	2040/846	124	250	2464	604
1250	225	2330/955	83	310	2723	863
1200	180	2510/1000	67	380	2957	1097

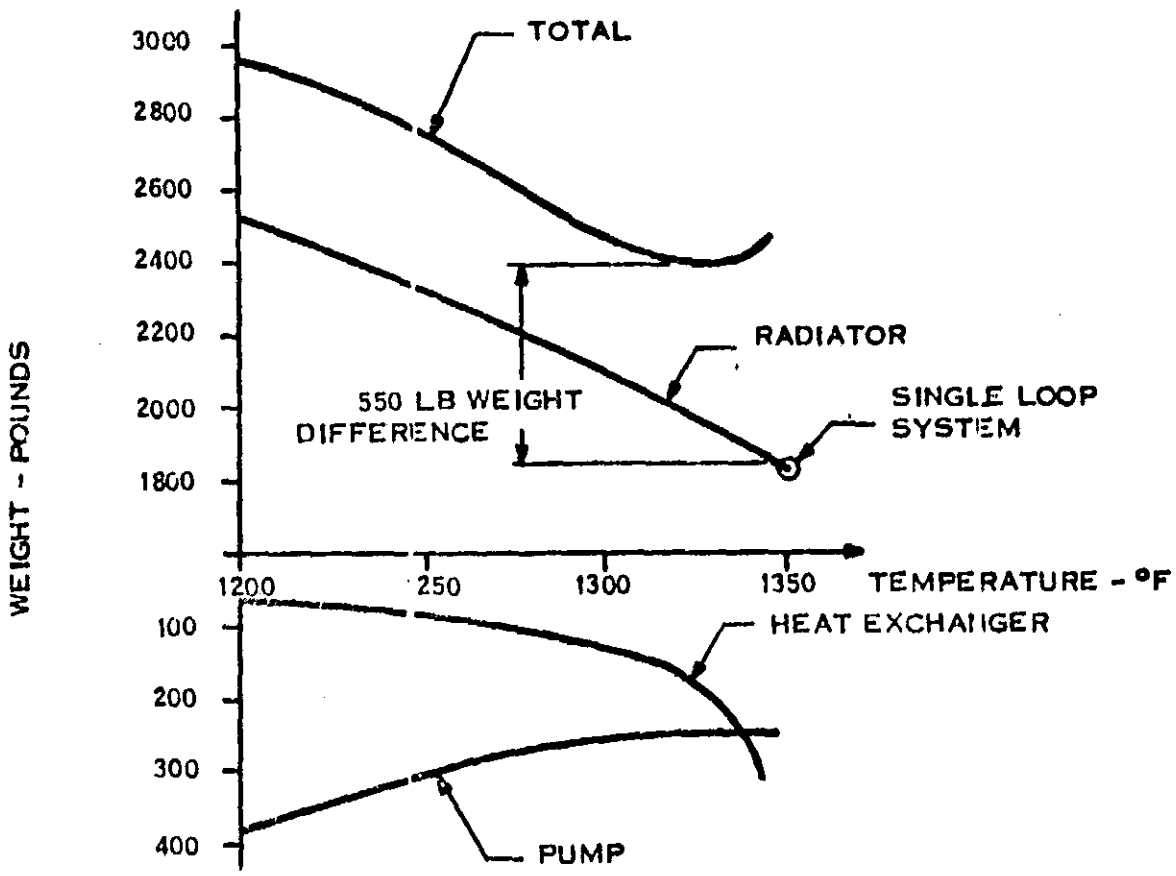

Figure 2-12. Two Loop System Weight Assessment

2.3.3 Activated Coolant Analysis in a Single Loop Primary Heat Rejection System

The use of a single loop heat rejection system for the thermionic reactor requires that consideration be given to the resulting distribution of activated coolant throughout regions containing radiation sensitive components. In order to estimate the magnitude of the problem, a geometrical and analytical model is identified which considers:

a. Bonded wet cell trilayer thermionic reactor

b. A single loop heat primary rejection system including feed lines, headers and radiator

c. Coolant activation (NaK-78)

d. Dose rates at selected points due to activated coolant distributed throughout the primary heat rejection system.

In addition to the activated coolant doses, a simplified approach was taken to make some estimate of the gamma doses to be expected from the reactor and from the secondary gamma sources in the mercury propellant, which is employed as gamma shielding.

2.3.3.1 Geometrical Model - An outline of the principle components under consideration and their relative locations are shown in Figure 2-13. The neutron shield thickness required to limit the integrated neutron dose to 10^{12} nvt is approximate and will be established in conjunction with future shield optimization studies. The propellant tank thickness is based upon the required volume for containment of the propellant.

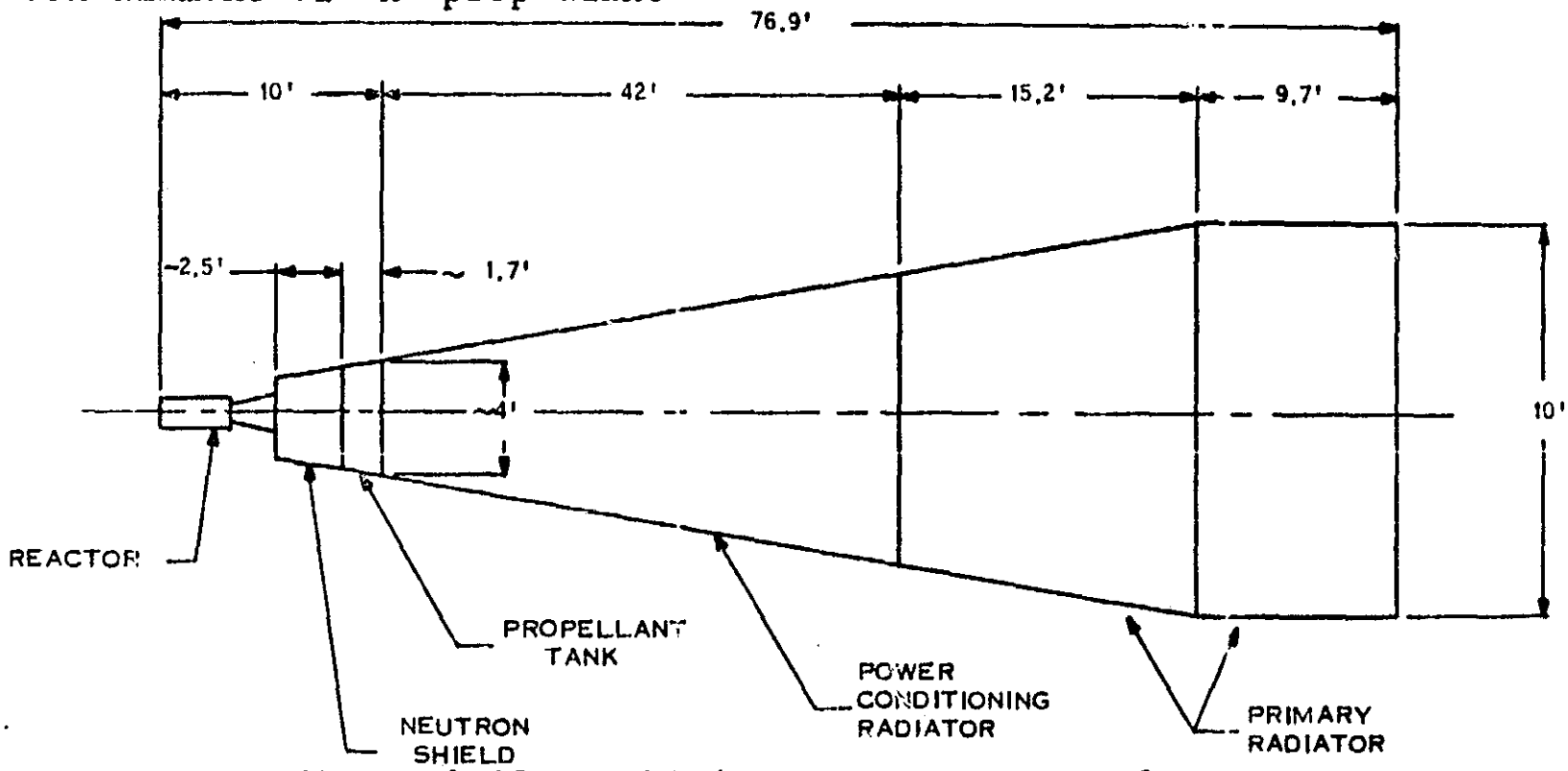

Figure 2-13. Vehicle Geometry Point of Departure Power Plant-Bonded, Wet Cell, Trilayer Flashlite Design

The various reactor regions and the coolant flow path through these regions are shown in Figure 2-14. In the coolant activation analysis it is assumed that the only significant activation occurs within these regions.

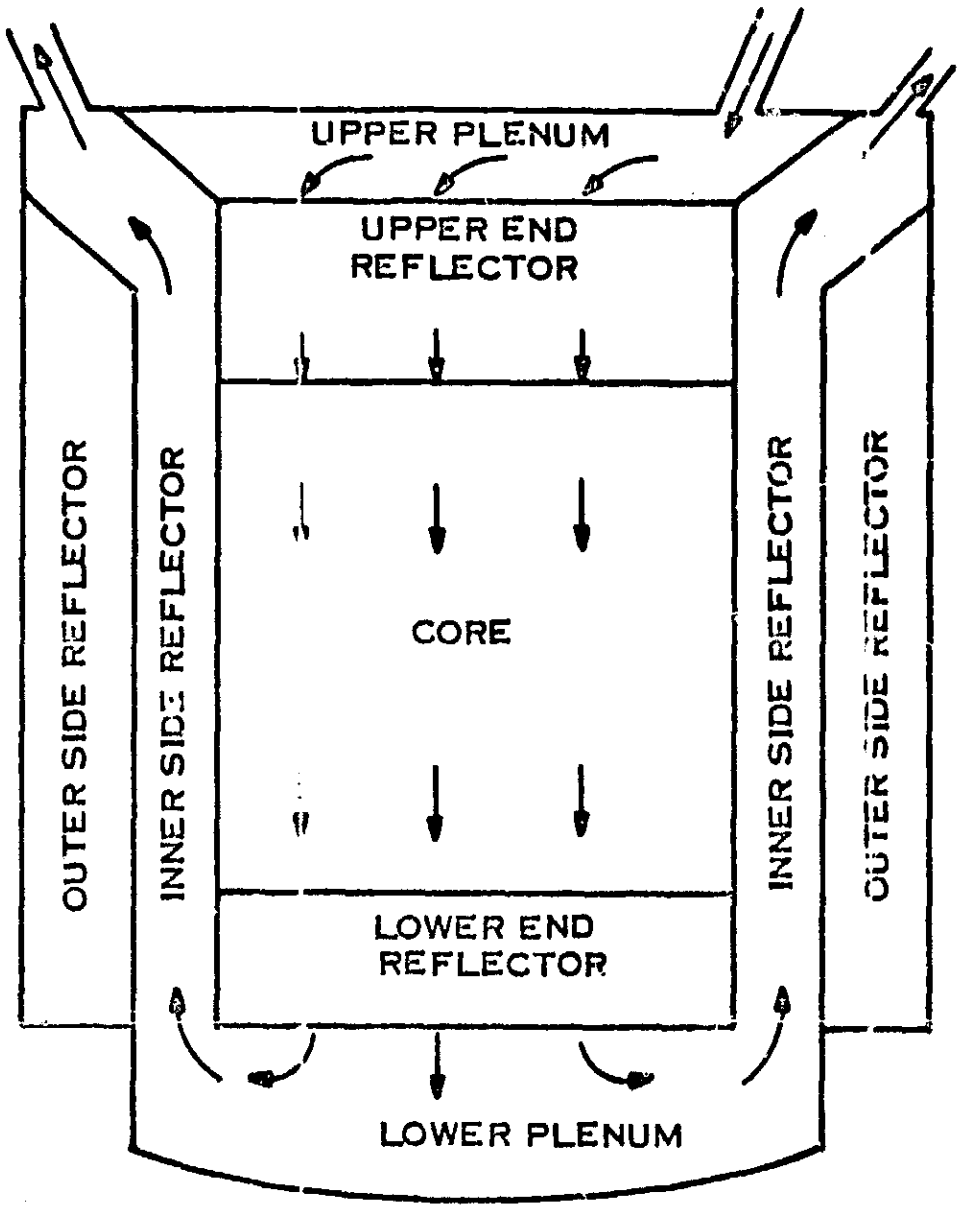

Figure 2-14. Wet Cell Bonded Trilayer Reactor Regions and Coolant Flow

In analyzing the gamma shielding contribution of the propellant, the loss of propellant with time must be accounted for. For calculational purposes, the propellant layer thickness, measured along the axis of the vehicle, was assumed to vary linearly with time during the two thrust periods. The propellant thickness as a function of time is given in Figure 2-15, along with the mission profile.

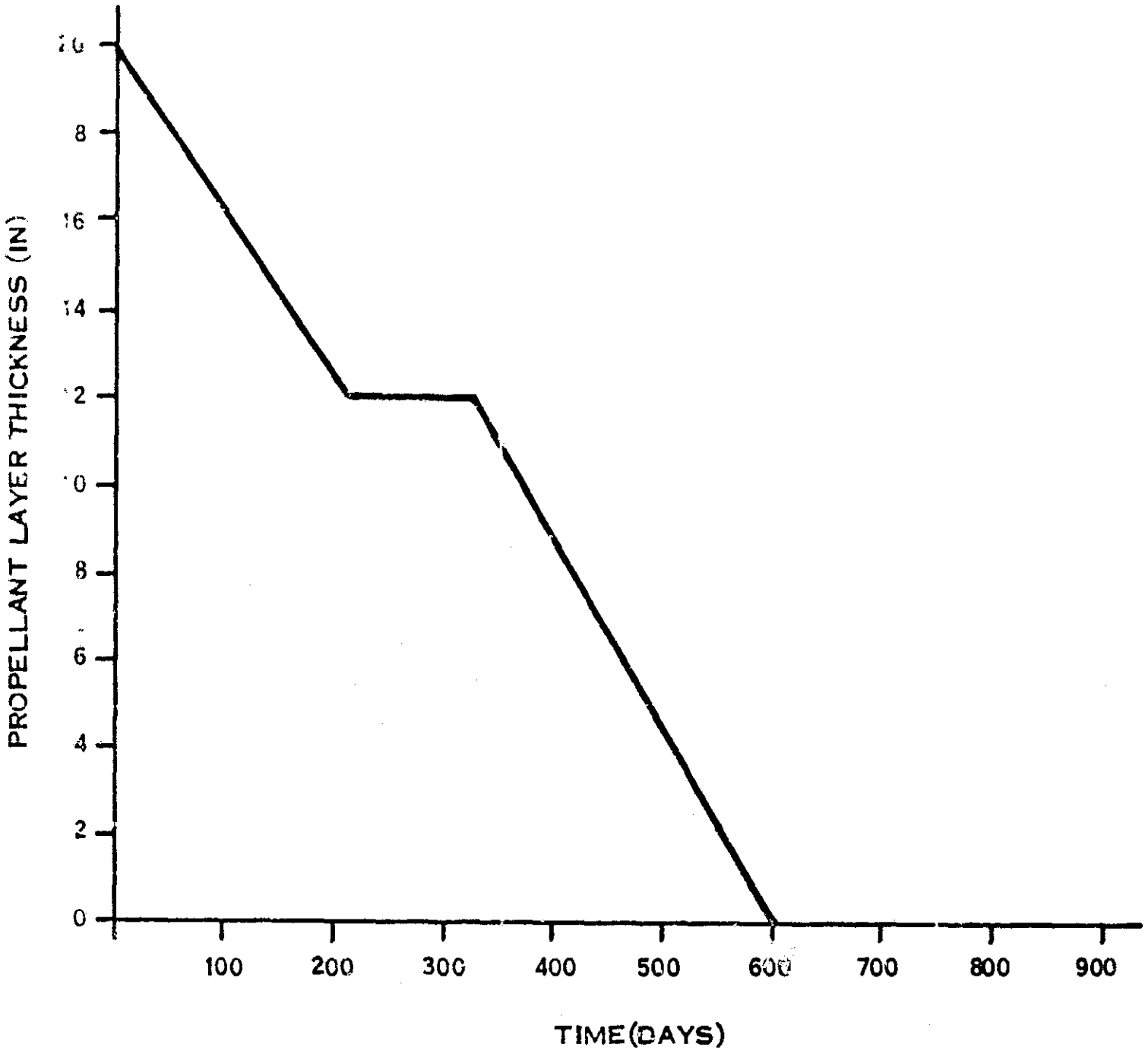

Figure 2-15. Mercury Propellant Thickness Decrease for Specified Mission Time Profile

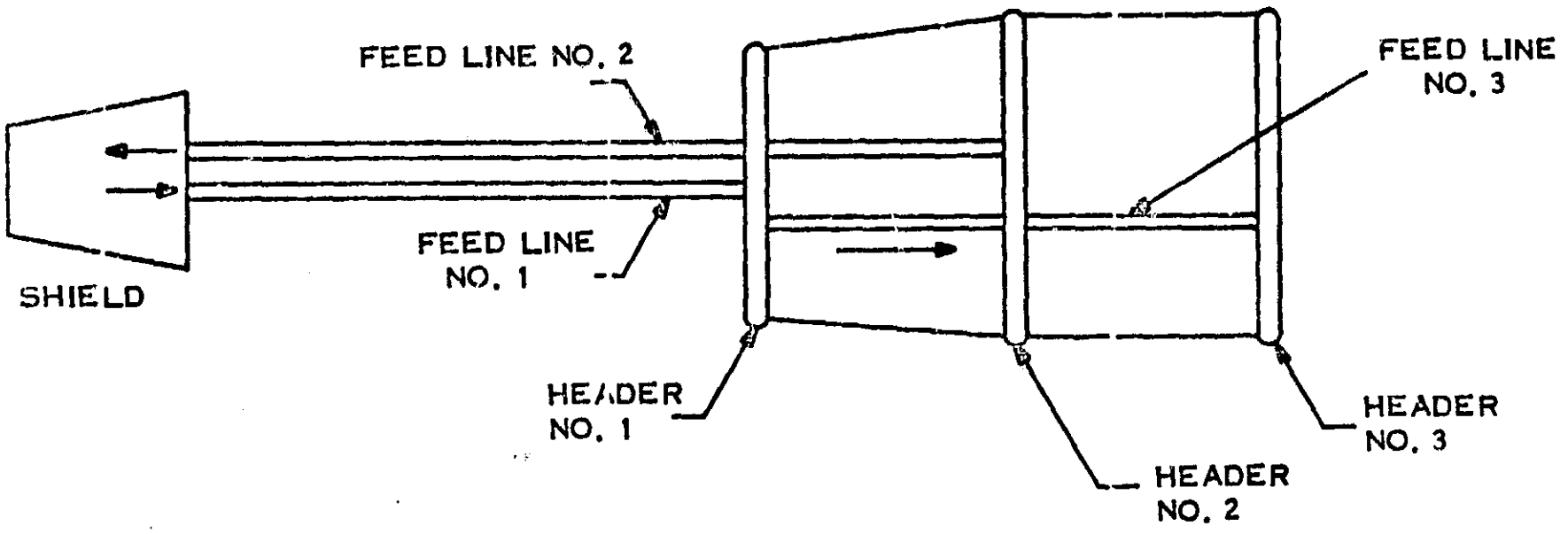

COMPONENT	INSIDE DIAMETER (IN.)
FEED LINE NO. 1	7.25
NO. 2	7.25
NO. 3	5.13
HEADER NO. 1	2.95
NO. 2	4.18
NO. 3	2.95

Figure 2-16. Activated NaK-78 Primary Coolant Radiator Geometry

2.3.3.2 Analytical Models

2.3.3.2.1 Coolant Activation

1. Analytical Model - The density of activated coolant nuclei at any given point in time and space depends upon the following factors:

a. Coolant activation cross sections

b. Activated nuclei decay constants

c. Neutron fluxes

d. Coolant distribution and flow rate throughout the system.

If attention is fixed upon a given small volume element, the instantaneous rates of production and loss of activated nuclei within the volume element are defined as follows:

$$\text{Production rate} = dV \int_0^{E_0} \Sigma_a(E)\,\phi(E, \vec{r})\,dE$$

$$\text{Loss rate} = \lambda A\,dV$$

where

dV = element of volume

$\Sigma_a(E)$ = activation cross section for neutrons of energy E

$\phi(E,\vec{r})dE$ = flux of neutrons with energies in the range dE about E at the point $\vec{r}$

λ = activated nuclei decay constant

A = density of activated nuclei

E_0 = maximum neutron energy.

The time rate of change of the density of activated nuclei can then be written:

$$\frac{dA}{dt} = \int_0^{E_0} \Sigma_a(E) \; \phi(E, \vec{r}) \, dE - \lambda A \qquad (2\text{-}1)$$

Since the coolant is in motion, the neutron flux seen by the coolant volume element is a function of time. Hence, the position coordinate, $\vec{r}$, can be written as a function of time. The time dependence of $\vec{r}$ will depend upon the volume element of coolant considered, since in general different elements will follow different paths. This fact would require solution of the Equation (2-1) for all possible paths and then averaging the results to obtain the average density of activated nuclei. The following assumptions were made in order to simplify the calculation.

It was assumed that the reactor/heat rejection system could be broken up into several regions and that within each region the neutron flux, as a function of position, could be replaced with its space averaged value. In addition, it was assumed that all elements of coolant spend the same time within any given region. The residence time in a given region was taken as the ratio of the coolant volume to the coolant volumetric flow rate in that region.

Equation (2-1) can now be rewritten, for example, for region "j", as:

$$\frac{dA_j}{dt} = \int_0^{E_0} \Sigma_a(E) \, \phi_j(E) \, dE - \lambda A_j \qquad (2\text{-}2)$$

The integration over energy in Equation 2-2 was recast into a summation over the multigroup neutron fluxes which had been calculated with a two-dimensional transport computer program. The final form of Equation 2-1 then becomes:

$$\frac{dA_j}{dt} = \sum_{g=1}^{G} \Sigma_g \, \phi_{gj} - \lambda A_j \qquad (2\text{-}3)$$

where

Σ_g = the g^{th} group averaged activation cross section

ϕ_{gj} = the g^{th} group neutron flux averaged over region j

Integration of Equation (2-3) gives:

$$A_j = \frac{1}{\lambda} \sum_{g=1}^{G} \Sigma_g \phi_{gj} + C_j e^{-\lambda t} \qquad (2\text{-}4)$$

The constants of integration, C_j, are determined by the requirement that A_j at the exit of region j is equal to $A_j + 1$ at the entrance to region j + 1.

In the steady state case, i.e., after several half lives of the activated nuclei, the density of activated nuclei at the exit from the reactor is:

$$A = \frac{1}{\lambda T} \sum_{j=1}^{J-1} \Delta t_j \left[\sum_{g=1}^{G} \Sigma_g \phi_{gj} \right] \qquad (2\text{-}5)$$

where

T = time for one complete cycle of the coolant

J = total number of regions

Δt_j = average time spent by coolant in region j.

Equation (2-5) also reflects the assumption that the neutron fluxes outside the reactor are small enough to be ignored. Hence, the summation over j does not include the radiator and radiator feed lines and headers.

2. Nuclear Data - In order to apply Equation (2-5) to a given problem, a knowledge of the neutron fluxes is required as well as the activation cross sections of all nuclear species included in the coolant, and the decay constants of any activated nuclear species.

The NaK-78 coolant contains two nuclear species which become activated when exposed to a neutron flux. They are Na^{23} and K^{41} which, upon neutron capture, become Na^{24} and K^{42}, whose decay constarts are 1.3×10^{-5} sec^{-1} and 1.55×10^{-5} sec^{-1}, respectively.

The group average activation cross sections used for these nuclides are given in Table 2-10. The coolant activation analysis was performed for the bonded wet cell trilayer in-core thermionic reactor configuration. The reactor regions are shown in Figure 2-12.

2.3.3.2.2 Coolant Activation Dose Rate

1. Analytical Model - The basic approach is based on the interaction cross sections of the emitted photons with the coolant itself, and with the containing structure were relatively small. The photons are emitted with energies of 1.37, 1.52 and 2.76 mev. These photons have mean free paths in the coolant of approximately ten inches and in the coolant containing structure of approximately two inches. Hence, in these materials, there will be very little photon scattering and, given the photon energies, pure absorption will be negligible. The scattering will reduce the energy of the scattered photons and hence their contribution to the total dose will be reduced. Ignoring photon scattering will act to slightly overestimate the dose rate. However, it was assumed that the coolant and containing structure was transparent to the photons.

TABLE 2-10. NEUTRON FLUXES AND ACTIVATION CROSS SECTIONS

Group	Group Energy Bounds (ev)	Sodium Activation Cross Section (barns)	Potassium Activation Cross Section (barns)
1	1.4×10^6 to 10.5×10^6	10^{-4}	10^{-3}
2	0.4×10^6 to 1.4×10^6	2×10^{-4}	2×10^{-3}
3	1×10^5 to 4×10^5	10^{-3}	10^{-2}
4	0.1×10^5 to 1×10^5	2×10^{-3}	2×10^{-2}
5	0.215 to 10^4	.04	.4
6	0.001 to 0.215	.53	1.3

The radiator feed lines and headers are described in Figures 2-13 and 2-16. The half lives of the activated Na and K are 15 and 12.4 hours, respectively, whereas the residence time in the radiator region is about one minute. The density of activated nuclei will not change appreciably during the residence time in the radiator region, and it was assumed that the activated coolant density was constant in this region.

With these considerations, the equation for the photon flux at a given point, due to photons of energy E, emitted by the i^{th} type of nuclear species within the volume element dV, can be written as:

$$d\phi(E) = \frac{S dV}{4\pi r^2} \qquad (2\text{-}6)$$

where

S = emission of photons of energy E, per unit time, per unit volume

r = separation distance between the element dV and the point at which the flux is to be calculated.

The source strength, S, is simply the product of the appropriate decay constant and the density of activated nuclei in the radiator region which is given by Equation (2-5). Hence,

$$d\phi(E) = \frac{\lambda A dV}{4\pi r^2} \qquad (2\text{-}7)$$

The total flux is obtained by integrating Equation (2-7) over that region of space containing activated coolant. The integration was performed by a computer program for the geometries describing the coolant distribution in feed lines, headers and conical radiators, as shown on Figure 2-16. This model calculates the flux at a given point due to photons that are emitted with directions that will bring them to the point of interest. However, photons emitted in other directions could be subsequently scattered to the point of interest. These scattered photons are not accounted for.

2. Nuclear Data - The photon energies and their numbers per decay for Na^{24} and K^{42} are given in Table 2-11.

TABLE 2-11. PHCTON PRODUCTION CHARACTERISTICS

Nuclide	Photon Energy (mev)	No. of Photons/Decay
Na^{24}	1.37	1.0
Na^{24}	2.76	1.0
K^{42}	1.52	0.2

The flux-to-dose conversion factors used are summarized on Table 2-12 (Reference 3).

TABLE 2-12. FLUX-TO-DOSE CONVERSION FACTORS

Photon Energy	Conversion Factor (r/hr per photon/cm^2-sec)
1.37	2.38×10^{-6}
1.52	2.56×10^{-6}
2.76	3.92×10^{-6}

2.3.3.2.3 Reactor Contribution to the Dose Rate

1. Analytical Model - Based upon previously calculated gamma doses with reactors as gamma sources (Reference 4), an estimate was made of the unshielded gamma dose rates to be expected from the subject reactor, at a point three feet from the propellant tank, as shown on Figure 2-13. It was assumed that only the propellant would significantly reduce this gamma dose. There will be some additional attenuation by the lithium hydride neutron shield, its structural material, and the propellant tank structure.

The unshielded dose rate will be proportional to the unshielded flux. The proportionality constant will depend upon the flux spectrum. Letting D_0 and ϕ_0 be the unshielded dose rates and photon fluxes, respectively:

$$D_0 = C\phi_0 \qquad (2\text{-}8)$$

Introduction of gamma shielding material will reduce the photon flux and also alter the photon spectrum. The latter effect will also alter the proportionality factor between gamma dose and photon flux. However, this effect was ignored, since no spectral data is available at present.

It was assumed that the uncollided photon flux at the point of interest is:

$$\phi_u = \phi_0 \; e^{-\Sigma x} \qquad (2\text{-}9)$$

where

ϕ_u = uncollided flux

Σ = propellant photon total cross section

x = propellant layer thickness.

The photon cross section is a function of photon energy, and the use of a single value requires that a flux spectrum average value be employed. Since the flux spectrum is unknown the conservative approach, choosing a value of the cross section near its minimum, is used.

In the case of a plane collimated source in an infinite media, the dose rate at a given distance from the source is:

$$D = BD_u \qquad (2\text{-}10)$$

where

B = dose buildup factor

D_u = dose rate due to the uncollided photons at the point of interest.

The quantity D_u is expressed in terms of the uncollided photons using the type of proportionality factor found above in Equation (2-8):

$$D_u = C\phi_u \qquad (2\text{-}11)$$

Combining Equations (2-10) and (2-11):

$$D = BC\phi_u \qquad (2\text{-}12)$$

Assuming that the same relationship between dose rate and uncollided flux holds for the case of the finite propellant shield, with the point of interest exterior to the shield:

$$D = BC\phi_o e^{-\Sigma x} \qquad (2\text{-}13)$$

where Equation (2-9) is used for expressing the uncollided flux, ϕ_u, in terms of the unshielded flux, ϕ_o. Using Equation (2-8), the dose rate is:

$$D = BD_o e^{-\Sigma x} \qquad (2\text{-}14)$$

This equation is used to estimate the dose rate at a position three feet from the propellant tank as a function of x, the propellant layer thickness. This can also be expressed as a function of time since the propellant is consumed during the two propulsion time intervals required in the mission, 210 days and 270 days. In order to estimate the integrated dose as a function of time, Equation (2-14) was rewritten as a function of time, assuming that the propellant layer thickness varied linearly with time during the propulsion periods.

At distances greater than three feet from the propellant tank, it was assumed that the dose rate varied inversely with the square of the distance from the reactor.

2. Nuclear Data - The unshielded dose rate, Do, was estimated to be 6×10^{3} rads/hr at a point three feet beyond the propellant tank. The macroscopic photon cross section, Σ, is $0.65\ cm^{-1}$, which corresponds to the mercury total photon cross section at a photon energy of about two Mev. The buildup factor is written in linear form, and is chosen to fit the buildup factor data for one Mev photons up to about four mean free paths. Beyond this energy, the selected form is a slight overestimate of the data. However, of the total accumulated dose from reactor photons during

the period of time before complete consumption of the propellant, about 90 percent is absorbed for a propellant layer thicknesses of four mean free paths (about six inches) or less. The expression used for the buildup factor, B, is

$$B = 1 + 0.35 \ \Sigma x$$

where

Σ = photon total cross section

x = propellant layer thickness.

2.3.3.2.4 Dose Rate from Secondary Photon Sources in the Mercury Propellant

1. Analytical Model - The large volume of mercury exposed to a neutron flux presents a sizeable source of secondary photons. Even though the neutron flux will have been attenuated by the lithium hydride neutron shield, and the photons will be attenuated to a considerable extent by the mercury itself, the magnitude of secondary gamma dose is established in these preliminary calculations.

In order to estimate this secondary photon source strength, the following procedure was adopted. The neutron flux level above one Mev was assumed to be such that the time integrated neutron flux, above one Mev, at a point three feet from the propellant tank would be 10^{12} nvt at the end of the mission. The weight optimized neutron shield required to provide this function will be defined later on in the program. Assuming that the neutron flux emerging from the propellant has a cosine angular distribution, an equivalent neutron surface source is derived. It was assumed that this source was constant over the rear face of the propellant tank, normal to the vehicle axis. It was further assumed that the neutron flux, above one Mev, was constant over the entire thickness of the propellant layer.

Given this surface source, the time integrated flux at a point three feet from the propellant tank, and on the axis of symmetry, is calculated. The integration is performed taking into account the changes in reactor power level with time, as shown in Figure 2-15, assuming that the propellant layer thickness changed linearly with time during the propulsion periods. The surface source was taken to coincide at all times with the outer surface of the propellant. The mercury propellant tank structure was assumed to have no effect upon the neutron flux, a pessimistic assumption.

The magnitude of the surface source, and therefore of the neutron flux above one Mev, was adjusted to that value which resulted in a value of 10^{12} nvt for the time integrated neutron flux at the three foot receiver point. The lithium hydride neutron shield will, of course, be designed to be consistent with this requirement.

Studies of deep penetration of fission spectrum neutrons in lithium hydride suggest that the flux of neutrons with energies above one Mev is of the same order of magnitude as the total neutron flux (Reference 5). Hence, the flux estimated as described above was taken to be the total flux. This flux, combined with a suitably averaged photon production cross section, will yield the secondary photon source strength throughout the propellant. The source strength is:

$$S\gamma = \Sigma_p \phi \qquad (2\text{-}15)$$

where

Σ_p = photon production cross section

ϕ = total neutron flux.

The differential dose rate at a point beyond the propellant tank, due to photons emitted from a small volume element of propellant is:

$$dD = \frac{S\gamma\, dV B}{4T_c R^2} \Sigma_a e^{-\Sigma r} \qquad (2\text{-}16)$$

where

dV = propellant volume element

B = dose buildup factor

Σ_a = photon energy absorption

Σ = propellant total photon cross section

R = distance from dV to the receiver point

r = path length within the propellant along R

The total accumulated dose was determined by integration of Equation 2-16 over the region of space occupied by propellant, and over time. The time integration included the mission variations in reactor power level, and in the propellant inventory. Equation 2-16 was programmed and then the spatial integration was performed by computer for a series of points in time. The time integration was performed graphically. The doses were calculated in this manner for a series of receiver points varying from 3 to 50 feet in axial distance from the propellant tank.

2. Nuclear Data - The photon energy absorption cross section in air, Σ_a, is assigned a value of 3.62×10^{-5} cm^{-1}. In principle, this cross section should be averaged over the photon flux spectrum at the receiver point. However, the photon spectrum is unknown and in order to be conservative, the value chosen for the cross section is selected at its maximum value.

The photon production cross section is estimated on the basis of measured values of the radiative capture and inelastic neutron cross sections of mercury. Since essentially all of the neutrons beyond the lithium hydride shield and the gamma shield propellant tank are expected to have energies above about 10 Kev (Reference 5), only cross sections above this energy are considered. The radiative capture cross section of mercury at 24 Kev has a reported value of about 0.2 barns, which decreases with increasing neutron energy. The inelastic scattering cross section has a threshold at about 0.16 Mev and reaches a peak value of about three barns at a neutron energy of four to five Mev.

The photon emission, per neutron interaction with mercury, is not well defined. Measurements indicate that in the case of thermal neutron capture in mercury, about three photons are emitted per capture, on the average. In the case of inelastic scattering, decay schemes of excited mercury nuclei indicate that several photons could be emitted, if a high enough energy level is excited. However, adequate information does not exist, especially in the form of cross sections for single level excitation, which would be required to make a more detailed estimate of the photon production rate.

As an order of magnitude estimate, an interaction cross section of two barns and a photon emission rate of three photons per interaction was assumed. The resulting value for Σ_p is 0.24 cm^{-1}.

2.3.3.3 Results

2.3.3.3.1 Coolant Activation - In order to display the reactor region and neutron energy dependence of the coolant activation, the quantity A_{gj} is given in Tables 2-14 and 2-15. The numbers refer to the 2330 kW(t) full power case. The quantity A_{gj} is defined as:

$$A_{gj} = \Delta t_j \quad \Sigma_g \quad \phi_{gj}$$

where

Δt_j = coolant residence time in reactor region j

Σ_g = activation cross section for energy group g

ϕ_{gj} = neutron flux in energy group g in reactor region j.

Thus, A_{gj} is the total number of activating interactions per unit volume due to neutrons in energy group g during transit through region j.

The group cross sections and fluxes were given in Table 2-10. The calculated residence times are given in Table 2-13.

A measure of the total contribution of each region to the density of activated nuclei is given in Table 2-16, where the quantity A_j is listed for each region. This is defined as:

$$A_j = \sum_{g=1} A_{gj}$$

The reactor regions are shown in Figure 2-14.

TABLE 2-13. BONDED WET CELL TRILAYER FLASHLIGHT REACTOR RESIDENCE TIMES

REGION	RESIDENCE TIME (Seconds)
Upper Plenum	.4
Upper End Reflector	.09
Core	.31
Lower End Reflector	.08
Lower Plenum	1.2
Inner Side Reflector	.8

TABLE 2-14. ENERGY GROUP AND REACTOR REGION CONTRIBUTIONS TO THE COOLANT ACTIVATION DENSITY

		A_{g_i} (Sodium)						
Energy Group	Group Energy Bounds (ev)	Upper Plenum	Upper End Reflector	Core	Lower End Reflector	Energy Group	Lower Plenum	Inner Side Reflector
1	1.4×10^{6} to 10.5×10^{6}	3.3×10^{5}	2.4×10^{5}	4.3×10^{6}	2.2×10^{5}	1	9.7×10^{5}	1.5×10^{6}
2	0.4×10^{6} to 1.4×10^{6}	1.6×10^{6}	1.0×10^{6}	1.6×10^{7}	9.0×10^{5}	2	4.9×10^{6}	6.3×10^{6}
3	$1.\times10^{5}$ to $4.\times10^{5}$	8.1×10^{6}	6.7×10^{6}	8.4×10^{7}	6.0×10^{6}	3	2.4×10^{7}	4.5×10^{7}
4	0.1×10^{5} to $1.\times10^{5}$	4.9×10^{7}	2.0×10^{7}	1.1×10^{8}	1.8×10^{7}	4	1.5×10^{8}	1.4×10^{8}
5	0.215 to 10^{4}	2.6×10^{8}	3.4×10^{8}	4.3×10^{8}	3.0×10^{8}	5	7.8×10^{9}	2.7×10^{9}
6	0.001 to 0.215	8.6×10^{9}	4.4×10^{7}	3.1×10^{6}	3.9×10^{7}	6	2.6×10^{10}	3.8×10^{8}

TABLE 2-15. ENERGY GROUP AND REACTOR REGION CONTRIBUTIONS TO THE COOLANT ACTIVATION DENSITY

		A_{gj} (Potassium)						
Energy Group	Group Energy Bounds (ev)	Upper Plenum	Upper End Reflector	Core	Lower End Reflector	Energy Group	Lower Plenum	Inner Side Reflector
1	1.4×10^{6} to 10.5×10^{6}	4.4×10^{5}	3.3×10^{5}	5.9×10^{5}	3.0×10^{5}	1	1.3×10^{6}	2.0×10^{6}
2	0.4×10^{6} to 1.4×10^{6}	2.2×10^{6}	1.4×10^{6}	2.3×10^{7}	1.2×10^{6}	2	6.7×10^{6}	3.8×10^{6}
3	$1.\times10^{5}$ to $4.\times10^{5}$	1.1×10^{7}	9.0×10^{6}	1.1×10^{8}	8.0×10^{6}	3	3.3×10^{7}	6.1×10^{7}
4	0.1×10^{5} to $1.\times10^{5}$	6.6×10^{7}	2.8×10^{7}	1.4×10^{8}	2.5×10^{7}	4	2.0×10^{8}	2.0×10^{8}
5	0.215 to 10^{4}	3.6×10^{9}	4.6×10^{8}	5.6×10^{8}	4.1×10^{8}	5	1.1×10^{10}	3.8×10^{9}
6	0.001 to 0.215	2.9×10^{9}	1.5×10^{7}	1.0×10^{6}	1.3×10^{7}	6	8.6×10^{9}	1.3×10^{8}

The photon emission rate per unit volume of NaK-78 coolant is given by the product of the decay constant, the density of activated nuclei and the number of photons per decay. In the case of sodium, each decay gives rise to two photons with energies of 1.37 and 2.76 Mev. In the case of potassium, 20 percent of the decays give rise to a single photon of energy 1.52 Mev. The emission rate density for each photon is:

$$S = n \lambda A$$

where

n = number of photons emitted per decay

λ = decay constant

A_j = density of activated nuclei

From Equation (2-5) and Table 2-16,

$$S = \frac{n}{T} \sum_j A_J \qquad (2\text{-}17)$$

Applying Equation 2-17 to the three photon energies discussed above yields the results given in Table 2-17.

The total integrated gamma dose, due to the activated coolant, are given in Table 2-18. The contributions to the doses, as well as the totals, from each of the radiator system components are listed for seven selected receiver points, also identified in Table 2-18. The reactor gamma dose contributions at each of the receiver points, and the total gamma dose are also presented in Table 2-18.

TABLE 2-16. REACTOR REGION CONTRIBUTIONS TO THE COOLANT ACTIVATION DENSITY

Reactor Region	A_j	
	Sodium	Potassium
Upper Plenum	1.13×10^{10}	6.6×10^{9}
Upper End Reflector	4.1×10^{8}	5.1×10^{8}
Core	6.5×10^{8}	8.4×10^{8}
Lower End Reflector	3.6×10^{8}	4.6×10^{8}
Lower Plenum	3.4×10^{10}	2.0×10^{10}
Inner Side Reflector	3.3×10^{9}	4.2×10^{9}
Total = $\sum_j A_j$	5.0×10^{10}	3.3×10^{10}

TABLE 2-17. COOLANT PHOTON SOURCE STRENGTHS

Photon Energy (mev)	Parent Nuclide	Source Strength (Photons/cm^3-sec)
1.37	Na^{24}	1.4×10^{9}
1.52	K^{42}	1.9×10^{8}
2.76	Na^{24}	1.4×10^{9}

The dose due to secondary photon sources in the propellant are negligible, and do not appear in Table 2-18. At a point three feet from the propellant tank, the total integrated gamma dose due to these secondary gammas is 160 rads.

The accumulated gamma dose, as a function of time, is shown in Figure 2-17 for two of the selected receiver points. The total dose, and the contribution from the activated coolant, are both represented by the same curve, since there are no other significant

contributors to the total dose. Figure 2-17 shows that the reactor contribution is never more than about five percent of the total integrated dose.

2.3.3.4 Conclusions - The integrated gamma dose due to activated coolant, given in Table 2-17, shows that a single loop heat rejection system cannot meet the 10^7 rad integrated dose limits, given the present power levels, mission duration, NaK-78 coolant. Even at receiver point number 1, the integrated dose from the activated coolant is a factor of 30 greater than the maximum allowable dose of 10^7 rads.

The results of the analysis of the reactor contribution to the gamma dose indicates that the propellant used during the first thrust period can be relocated at the payload (aft) end of the vehicle without any significant increase in the integrated gamma dose.

The reactor contribution to the integrated dose at receiver point 1 (three feet behind the mercury propellant tank) is slightly above the allowable level for a full 300 days in Jupiter orbit. However, several 16-day orbits appear to be attainable without exceeding the 10^7 rad integrated dose limit. It therefore appears that no permanent gamma shielding will be required in a two-loop system.

2.4 SYSTEM ANALYSIS DEVELOPMENT

A computer program is being written to assist in the design and optimization of the thermionic reactor power systems and spacecraft for specified sets of conditions. A preliminary detailed logic procedure for the basic system design sequence has been formulated and is being refined with continuing analyses. Figure 2-18, a simplified representation of that procedure, shows the current sequence of calculation and the major blocks of analyses which will comprise the program. The design sequence directs the analysis from component to component, providing the necessary input and processing the output of each component model. It also provides estimates of certain parameters to permit continuing closed form solutions and directs iterations with re-estimates of those parameters as necessary. The dashed lines on the diagram of Figure 2-18 are examples of the iterations which may be necessary when the power conditioning radiator is placed directly behind the shield. Estimates of the main radiator feed line length and the average length of a low voltage cable are needed before the power conditioning radiator is sized. When the radiator is sized and the feed lines and cable lengths computed, iteration may be necessary to equalize the estimated and computed

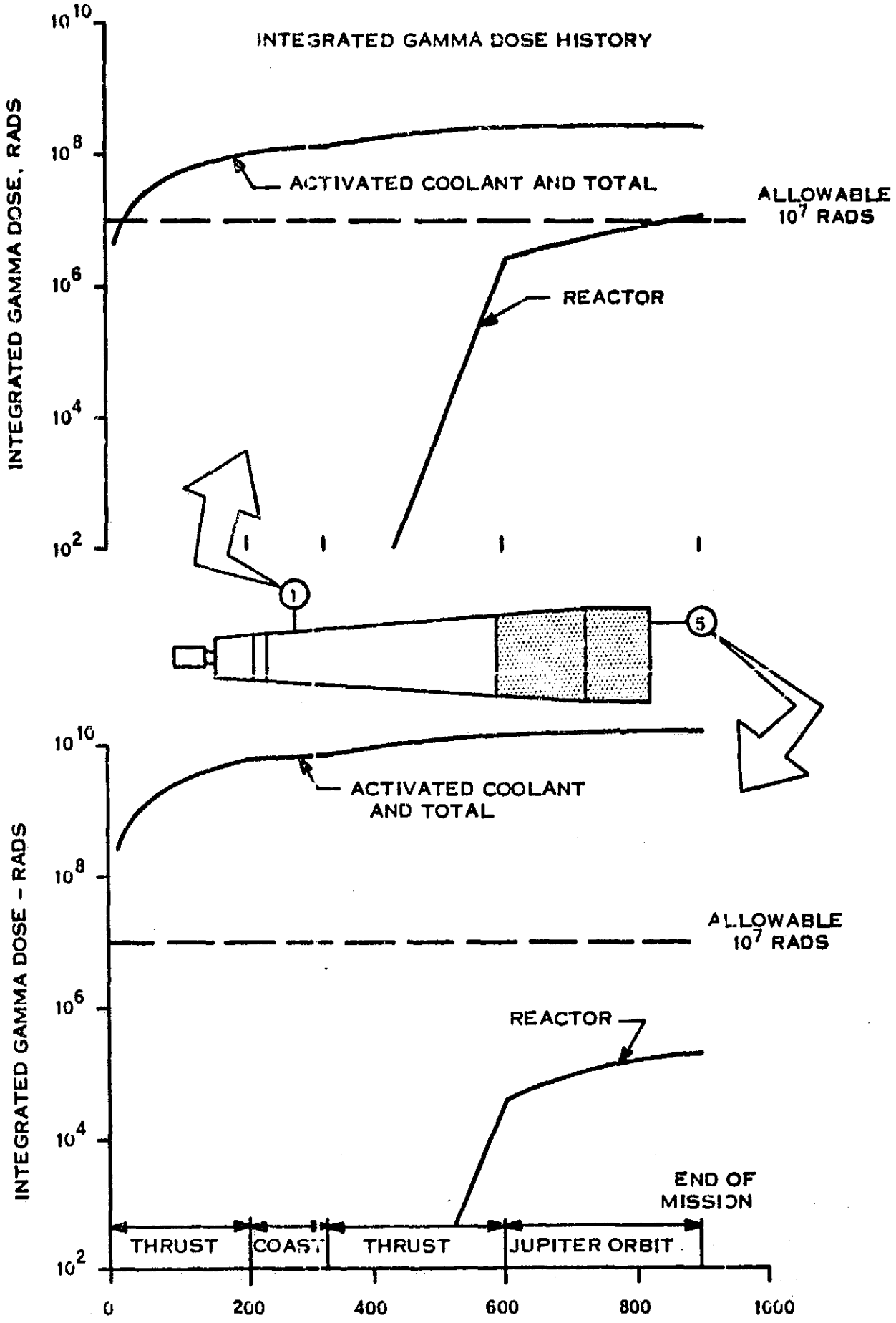

Figure 2-17. Integrated Gamma Dose History

TABLE 2-18. INTEGRATED GAMMA DOSE

- NAK-78 COOLANT
- 900 DAY MISSION

SOURCE \ RECEIVER POINT	INTEGRATED GAMMA DOSE RADS X 10^{-8}						
	1	2	3	4	5	6	7
RADIATOR	.002	.006	.014	.108	.086	.092	.079
HEADER 1	.297	1.22	3.91	129.8	.969	1.034	.859
HEADER 2	.475	1.25	2.37	5.40	9.34	10.64	12.30
HEADER 3	.180	.366	.580	1.15	147.3	38.00	28.40
FEED LINE 1	.924	.960	.769	.383	.023	.021	-
FEED LINE 2	.925	.974	.849	.739	.071	.073	-
FEED LINE 3	.004	.012	.031	.170	.138	.263	-
SUBTOTAL	2.807	4.788	8.523	137.750	157.927	50.130	41.638
ACTIVATED COOLANT REACTOR	0.112	0.013	0.007	0.005	0.002	0.002	0.002
TOTAL INTEGRATED GAMMA DOSE	2.919	4.801	8.530	137.755	157.929	50.132	41.640

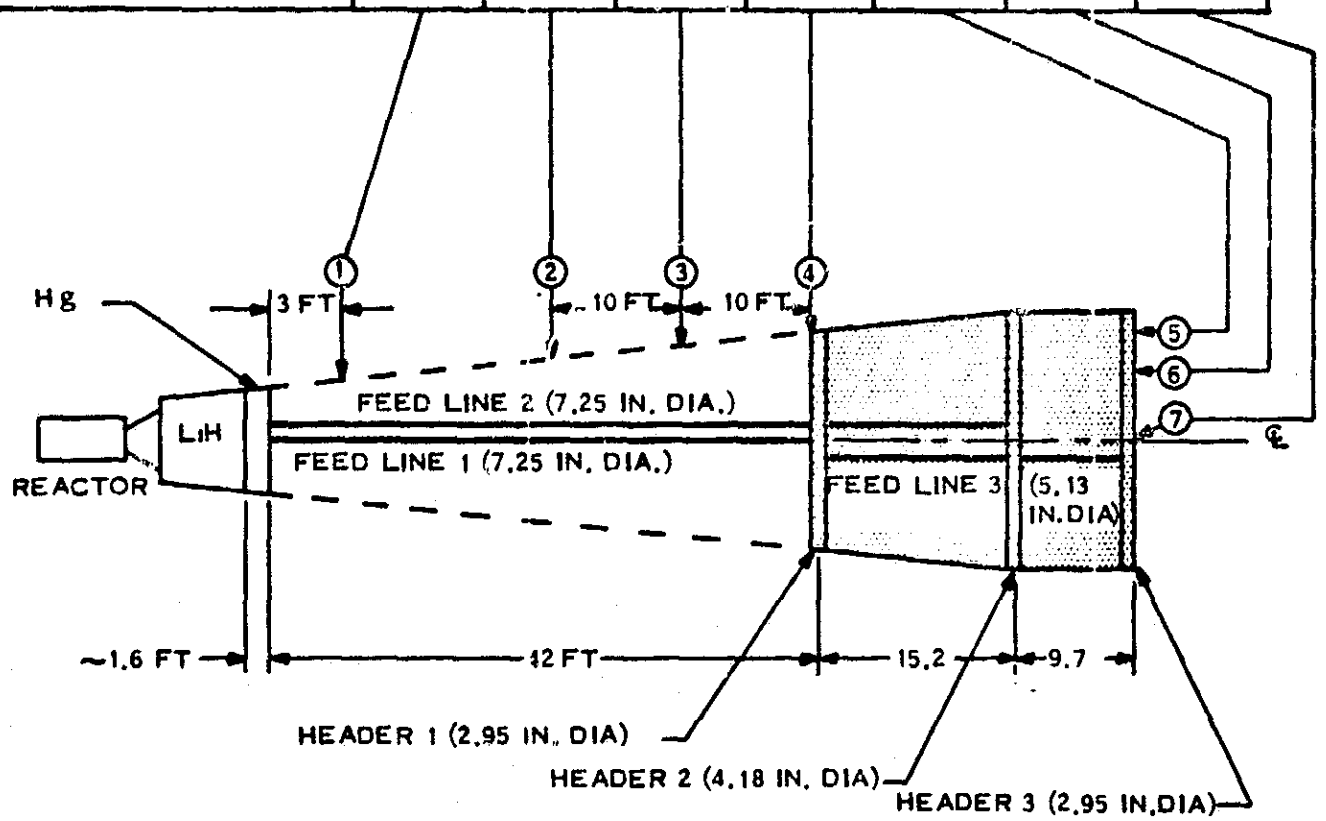

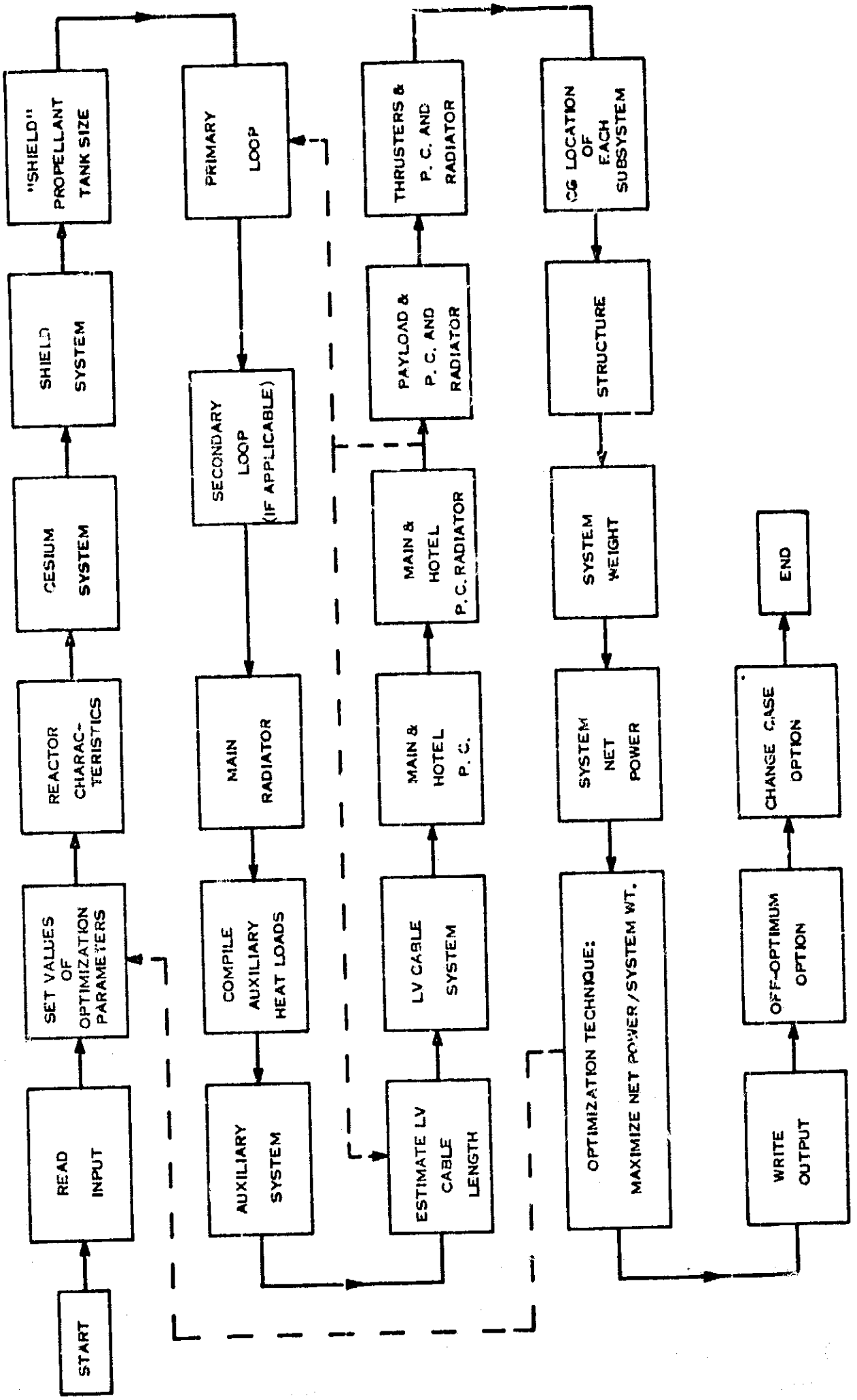

Figure 2-18. Simplified Logic Diagram for Computer Program

values. The dashed line leading from the optimization block represents the iterations required with revised values of the optimization parameters in order to maximize the net power per unit weight of the system.

Each component block will be a mathematical model to utilize input boundary conditions to compute the size and weight of the component, determine the output conditions of the component, and to determine the energy balance for each component.

2.5 MISSION OPERATIONS

No analysis has been accomplished in the area of Mission Operations during the first quarter of this study. Areas of future concern include:

a. Mission Operations

   1. Pre-launch Operations
   2. Flight Operations

b. Mission Analysis

c. Aerospace Nuclear Safety.

3. CONCLUSIONS

The following conclusions are identified:

1. Coolant activation analysis of a power plant based on a single loop, primary heat rejection system demonstrates that the total integrated gamma dose from the activated coolant exceeds the allowable integrated dose of 10^7 rads by up to several orders of magnitude. This evaluation was based on the point of departure power plant utilizing the bonded, wet cell flashlite reactor. It is concluded that a two-loop primary heat rejection system will be required for power plants based on this reactor.

2. The weight penalty of a two-loop heat rejection system (compared to a one loop system) is approximately 550 pounds, including the weight associated with the heat exchanger, pump, and decreased primary radiator temperature (increased area).

3. A spacecraft flight fairing length of about 80 to 90 feet will be required on the Titan III C/7 launch vehicle (10 foot diameter). If this shroud is jettisoned in Earth orbit, the payload weight penalty will be 100 percent of the shroud weight, or up to 4600 pounds. This will limit the payload to about 25,400 pounds for launch into a 625 nm Earth circular orbit. It is concluded therefore that using the shroud as a payload thermal shield to prevent coolant freezing in Earth orbit prior to power plant startup is not a feasible approach.

4. While operating in Earth orbit, the power conditioning radiator temperature will be 212°F, which is 37°F above the maximum allowable (currently assumed at 175°F). To limit electronic component temperatures to the maximum allowable of 200°F, under these assumptions, the system power level must be maintained below 77 percent of full power during initial spiral out from Earth orbit. Alternately, it may be acceptable to operate the electronics equipment above 200°F (about 230°F) for the 50 to 70 days required to spiral out to escape velocity from Earth orbit.

5. Definition of the payload and communicatons subsystems has been completed. The total weight of these subsystems, including data handling components, is approximately 262 pounds. Since 2200 pounds has been allocated for the payload, an additional 1940 pounds is available for payload growth.

6. At least 800 watts(e) of the 100 watts(e) allocated for payload and communications will be available to the communications subsystem, providing a data rate of 10^4 bits/second from Jupiter orbit.

4. RECOMMENDATIONS

The following recommendations are identified based upon the results and conclusions of the first three months of the Thermionic Spacecraft Design Study:

1. The use of a two-loop primary heat rejection system is recommended in conjunction with the bonded wet or dry cell flashlite reactor. Cursory additional evaluations are recommended for the pancake and the externally fueled thermionic reactor approaches, but no use of a single primary heat rejection loop are recommended unless orders of magnitude improvement in the reduction of NaK-78 coolant activation are identified.

2. During ascent to Earth orbit, the flight fairing should be ejected at approximately 280 seconds after launch. Alternate methods of thermal control to prevent coolant freezing while in Earth orbit (prior to plant start-up) should be investigated. Consideration should be given to multifoil or Mylar insulation.

3. Mission analysis should be completed to define the relative advantages and disadvantages variously associated with either operating the power plant at reduced power level during spiral-out to Earth escape ($\sim 300^{\circ}R$ sink temperature) or allowing the on-board electronic components to operate at higher temperatures ($\sim 230^{\circ}F$) during the 50 to 70 days required for this mission phase. Such analysis is beyond the scope of this study.

4. Additional effort is required to firmly define the total effective utilization of the current one metric ton science and communications subsystem payload ($\sim$ 2200 lbs), as well as the need for payload and communications subsystem power electric levels above 1 kW(e). Such higher power levels, up to 5 kW(e) to 10 kW(e), can probably be accommodated if required. Such improved definition is beyond the scope of this study.

5 SYMBOLS AND NOTATION

5.1 RADIATOR ARMOR CALCULATION

t = radiator armor thickness, cm

ρ_m = meteoroid density, gm/cm^3

m = meteoroid mass, gm

v = meteoroid velocity, km/sec

α = empirical coefficient

β = empirical exponent

$P_{(0)}$ = non-puncture probability

ϕ = cumulative meteoroid flux, number particles/m^2sec

A = projected vulnerable area of the spacecraft (radiator), m^2

T = exposure time, sec

ASSUMED VALUES:

$\bar{\rho}_m$ = 0.5 g/cm^3 $\quad$ α = 6.62×10^{-15}

V = 20 km/sec $\quad$ β = 1.34

T = 7.2×10^7 sec (20,000 hr) $\quad$ $P_{(0)}$ = 0.95

5.2 POWER CONDITIONING RADIATOR CALCULATIONS

η_F = fin efficiency

L = fin length

$m = \sqrt{2h/k\delta}$

h = equivalent surface heat transfer coefficient

k = thermal conductivity of the fin material (assumed to be 100 B/hr-ft-^oF for aluminum alloy)

δ = fin thickness (0.15 inch)

η_o = overall surface effectiveness

A_f = fin area

A = total radiator area

q = heat rejection weight

σ = Boltzman's constant

ξ = surface emissivity

T_R = max. radiator surface temperature

T_S = equivalent sink temperature

6. REFERENCES

1. GE Proposal No. GENSP-K-68-071, "Design Study for a Thermionic Reactor Power System for a Nuclear-Electric Propelled Unmanned Spacecraft", Volume 1, October 21, 1968.

2. Terrill, W., Notestein, J., "Radiator Design and Development for Space Nuclear Powerplants," Vol. II, 64SD224B, General Electric Missile and Space Division, Valley Forge, Pa., February 1964.

3. Miscellaneous Data for Shielding Calculations; compiled by John Moteff, General Electric Company; APEX-176; December 1, 1954.

4. Low Acceleration Space Transportation System Study; Final Report, Volume II, Technical Report; General Electric Company; ANSO Document Number 6300-260-2; September 1967.

5. Fission Neutron Attenuation in Lithium - 6, Natural Lithium Hydride, and Tungsten; Gerald P. Lahti: Lewis Research Center.

The total accumulated dose was determined by integration of Equation 2-16 over the region of space occupied by propellant, and over time. The time integration included the mission variations in reactor power level, and in the propellant inventory. Equation 2-16 was programmed and then the spatial integration was performed by computer for a series of points in time. The time integration was performed graphically. The doses were calculated in this manner for a series of receiver points varying from 3 to 50 feet in axial distance from the propellant tank.

2. Nuclear Data - The photon energy absorption cross section in air, Σ_a, is assigned a value of 3.62×10^{-5} cm^{-1}. In principle, this cross section should be averaged over the photon flux spectrum at the receiver point. However, the photon spectrum is unknown and in order to be conservative, the value chosen for the cross section is selected at its maximum value.

The photon production cross section is estimated on the basis of measured values of the radiative capture and inelastic neutron cross sections of mercury. Since essentially all of the neutrons beyond the lithium hydride shield and the gamma shield propellant tank are expected to have energies above about 10 Kev (Reference 5), only cross sections above this energy are considered. The radiative capture cross section of mercury at 24 Kev has a reported value of about 0.2 barns, which decreases with increasing neutron energy. The inelastic scattering cross section has a threshold at about 0.16 Mev and reaches a peak value of about three barns at a neutron energy of four to five Mev.

The photon emission, per neutron interaction with mercury, is not well defined. Measurements indicate that in the case of thermal neutron capture in mercury, about three photons are emitted per capture, on the average. In the case of inelastic scattering, decay schemes of excited mercury nuclei indicate that several photons could be emitted, if a high enough energy level is excited. However, adequate information does not exist, especially in the form of cross sections for single level excitation, which would be required to make a more detailed estimate of the photon production rate.

As an order of magnitude estimate, an interaction cross section of two barns and a photon emission rate of three photons per interaction was assumed. The resulting value for Σ_p is 0.24 cm^{-1}.